THE FLORIDA STATE UNIVERSITY

COLLEGE OF ARTS AND SCIENCES

UNDERSTANDING THE 21ST CENTURY PROJECTION OF THE WET SEASON OVER THE SOUTHEASTERN UNITED STATES

By

CHRISTOPHER M. SELMAN

A thesis submitted to the
Department of Earth, Ocean, and Atmospheric Sciences
in partial fulfillment of the
requirements for the degree of
Master of Science

Degree Awarded:
Summer Semster, 2012

Christopher Manuel Selman defended this thesis on April 3rd, 2012.

The members of the supervisory committee were:

Vasubandhu Misra
Professor Directing Thesis

Mark Bourassa
Committee Member

Lydia Stefanova
Committee Member

Zhaohua Wu
Committee Member

The Graduate School has verified and approved the above-named committee members, and certifies that the thesis has been approved in accordance with university requirements.

TABLE OF CONTENTS

LIST OF TABLES

LIST OF FIGURES

ABSTRACT

This study analyzes projections of summer precipitation over the Southeastern United States under the A2 climate scenario using the Community Climate System Model Version 3 (CCSM3), and the Regional Spectral Model (RSM) forced with CCSM3 output. The CCSM3 projects a dipole in precipitation, while the RSM projects a universal drying of the Southeast. The difference in patterns of projected rainfall is explained through the RSM's depiction of the diurnal variance of precipitation, which according to observations can account for up to 40% of total seasonal variance in precipitation. The CCSM3 pattern is attributed to an exaggeration of the "upped-ante" mechanism, whereby the atmospheric boundary layer (ABL) moisture required for convection to occur increases in a warmed environment. Also contributing to the drying of both models is an expansion of the North Atlantic subtropical high (NASH).

CHAPTER ONE

INTRODUCTION

1.1 - The Southeastern United States

For stakeholders and non-scientists alike, climatology occupies an increasing interest in the public discourse. Reports on global climatology from the Intergovernmental Panel on Climate Change (IPCC) recently popularized by the media, have done much to pique interest. However, people have become aware that climate change, while a global phenomenon, has distinct regional impacts. While one region may experience warming, another may experience cooling. Also of interest is what happens to rainfall under a changing climate in different regions of the globe. Studies of rainfall change exist, but few seek to understand differing projections between climate models. We choose to assess and understand differing projections of rainfall change in two climate models by looking at rainfall projections of future climates in the Southeastern United States.

We chose this region because the Southeast is an agricultural hotbed. Part of this stems from the fact that the Southeast is climatologically the wettest region in the contiguous United States (Chan et al. 2010). From 1991 to 1995 Alabama, Florida, Georgia, and South Carolina alone had a mean industry value of over 3 billion dollars for crops that included peanuts, tomatoes, cotton, tobacco, corn and soybeans (Hansen et al. 1998). This value has undoubtedly grown since, likely due to an increase in population leading to an increase in demand. Crop growing in the Southeast is largely rain fed. If climate change in this region has any impact on rainfall, there could be dire consequences for the crop industry. Therefore, we choose to look at how rainfall might change in the late 21st century.

To narrow our window of study down further, we choose to look at changes in rainfall in the Southeast summer. This season is chosen as it is the wet season for the region, and the region relies on summer rains to replenish groundwater and irrigate crops (Misra et al. 2011). Changes in this rainfall supply can have disastrous effects, especially given that the population in the Southeast is growing at a very fast

rate. Increased stress on aquifers coupled with a reduced replenishment rate may deplete aquifers, strain surface water resources and allow for saltwater intrusion into the shallow aquifers of the Southeast (Karl et al. 2009). Because of this, it is important to have an idea of what to expect and why to expect it. Knowledge of future summer climate can then be used to mitigate the impact of future climate scenarios. However, before studying how rainfall has been changing in the Southeast we must seek to understand the rainfall of the Southeast in summer, which is introduced below.

1.2 – Diurnal Rainfall in the Southeast

In specific, we choose to look at diurnal rainfall, as in the Southeast diurnal rainfall is seen to account for a large fraction of summer seasonal rainfall (this will be shown in Chapter 3). It is also noted that in the summer, the Southeast has the strongest local diurnal maximum in the United States (Carbone and Tuttle 2008). Diurnal rainfall is the daily pattern of maximum and minimum rainfall, and is modulated by convective activity and light rainfall from stratiform clouds (Wallace 1975). Both convective activity, and stratiform rainfall occur as a response to the diurnal cycle in solar heating. In the coastal regions of the Southeast, local sea breeze effects primarily drive diurnal variations in rainfall (Schwartz and Bosart 1979), and over mountainous terrain development of storms from sensible heating of terrain drives the diurnal pattern (Parker and Ahijevych 2007). Generally, the peak of the diurnal rainfall pattern occurs in afternoon hours, though Parker and Ahijevych (2007) noted that westward propagation of systems over complex terrain delays the timing of the diurnal maximum by a few hours in areas east of the Appalachians.

Given the Southeast's immediate proximity to the Gulf of Mexico and Atlantic Ocean it is no surprise that sea breezes are a significant component of regional rainfall. Sea breezes, in short, arise from the differing heat capacities of land and ocean (Biggs and Graves 1962). The specific heat capacity of land is lower than that of water, and as a result differences in temperatures above the two surfaces exist. The temperature differences modify the density of air above the surface and establish a pressure gradient. Flow between the dissimilar densities produces a

breeze effect. Given that the sea breeze is intimately died to the diurnal variation in temperatures (Biggs and Graves 1962), it is not surprising that sea breezes are intimately tied to diurnal rainfall, as noted in Schwartz and Bosart (1979.)

As for why we should expect sea breeze to play a role in initiating convection, we look to analysis by Atkins et al. (1995). In one study, it was noted that the density current creating sea breeze flows is analogous to the establishment of a sea breeze front (Simpson 1987). Development of storms from onshore flow of the sea breeze is strengthened by merging of horizontal convective rolls flowing nearly parallel to the sea breeze front and the sea breeze front itself (Atkins et al. 1995). Horizontal convective rolls are regions of vertical instability, rotating oppositely from one another (LeMone 1973). Horizontal convective rolls, merging with the sea breeze tend to enhance convection associated with storms coming onshore, which as mentioned above, is the primary contributor to the diurnal rainfall in the primarily coastal Southeast.

1.3 – Climate Change in the Southeast

One potential driver of climate change in the Southeast is sea surface temperature (SST) changes in remote oceans. Current studies propose that sea surface temperatures will likely warm, especially in oceans that are not near the Southeast, in the coming decades (Rauscher 2011). Warming of these remote oceans is understood to have pronounced impacts on the Southeast (Xie et al. 2010). A primary driver of this warming in SSTs is thought to be increasing concentrations in atmospheric greenhouse gases (GHGs) (Christensen et al. 2007). These changes in SST have varied influences on climates around the globe, but tend to affect rainfall negatively in the Southeast (Chiang and Sobel 2002). It is not unusual to assume that warming SSTs will have an impact on the climatology of the region, given that it is bordered by the Atlantic Ocean. The mechanisms by which changing SSTs influence climate in the Southeast are many and varied. One such mechanism is the altering of cloud cover through warming of SSTs (Wang and Enfield 2001.)

One interesting facet of the Southeast is that it exhibits a general cooling in surface temperatures in spring and winter (Portmann 2009). Fig. 1.1 (their Fig. 1) shows a map from Portmann et al. 2009 demonstrating this trend disparity. Several

studies were performed to demonstrate this. One explanation of the observed cooling of surface temperatures, proposed by Robinson et al. (2002), involves warming of tropical SSTs. Rising tropical SSTs account for additional cloud cover, as additional precipitable water evaporates from the Gulf of Mexico (as well as surrounding oceans.) As a result, relative humidity is increased in the region, and clouds are more likely to form. When this happens, incoming solar radiation is blocked, and temperatures at the surface will generally decrease.

Misra et al. (2012) discussed observed linear trends in temperature observations in the Southeast are related to land use changes. Land use represents a significant contribution to climate change (DeGaetano et al. 2002). As analysis of observations reveals in the study, there is a warming trend in minimum temperature, within the 5% confidence interval, in the Southeast over urbanized areas. Maximum summer temperatures on the other hand are shown to be negative, but not statistically significant, over urbanized areas. This is consistent with the idea of the urban heat island (Karl et al. 1988). Misra et al. (2012) further showed that irrigation also has a minor impact on observed summer minimum and maximum temperature trends in the Southeast. Minimum temperatures are warmed, while maximum temperatures are cooled when irrigation is employed. The reason for this cooling is an increase in evaporation during the day from the added moisture, which cools the region.

A number of studies have looked into the change in summer precipitation over the Southeast. A study by Ortegren et al. (2011) showed that the Southeast is less prone to prolonged drought in a future climate. Other studies hypothesized that changes in the North Atlantic subtropical high (NASH) play a strong role in seasonal rainfall variability (Li et al. 2011; Christensen et al. 2007). As seen in Fig. 1.2 from Li et al. (2011, their Fig. 2), 850-hPa geopotential heights show a strong decadal shift, bringing enhanced subsidence to the Southeast. As a result, the variability in summer rainfall is increased, leading to a greater number of extreme event years of drought and flood. Katz et al. (2003) showed that circulations associated with the NASH are strongly correlated with precipitation.

There is a noticeable change in Southeast summer precipitation. Li et al. (2011) demonstrated a pronounced variability of summer precipitation over the Southeast. The study verifies that movement of the NASH is responsible for as much as -0.3 to -0.5 mm/day change in rainfall. This change is calculated by correlating the linear regression of rainfall in the late 20th and early 21st centuries with the latitude of the western ridge of the NASH. This correlation is different from results seen in the mid 20th century by a significant amount, as much as a difference of 4 mm/day in some cases. The study concluded that over recent decades the variability of the NASH has become a significant driver in Southeast summer rainfalls.

Another way in which precipitation can be modified in the Southeast involves a mechanism known as the "upped-ante" mechanism (Neelin et al. 2003.) In a warmed tropospheric environment the amount of atmospheric boundary layer (ABL) moist static energy required to initiate convection increases (Chiang and Sobel 2002). In general, the source of this extra moist static energy comes from ABL moisture. If ABL moisture is abundant (e.g., over the oceans) meeting the moisture "ante" to initiate convection is not problematic, and the region will have increased rainfall. On margins of these convective regions we generally tend to see a reduction in precipitation. This is because low-level flow across these margins comes from a typically nonconvective source. As a result the required amount of moist air in the boundary layer required to initiate convection is not obtained, and thus precipitation for the region tends to decrease. In this study, the Southeast can be considered to be on the edge of a convective margin given its proximity to the tropics. Fig. 1.3 (Neelin et al. (2003) Fig. 3) summarizes the upped-ante mechanism.

1.4 – Comparing Regional Change to Global Change

There are a number of important considerations we must take into account when comparing regional climate change in the Southeast to global climate change. Perhaps the biggest issue is the inability to adequately resolve the region. For instance, some global climate models may dedicate as little as one grid cell to peninsular Florida (Misra et al. 2011). Rather than resolving the area as land, large swaths of land are treated as ocean as seen in Fig. 1.4 (their Fig. 6.1). As a consequence, global models are likely unable to faithfully recreate the precipitation

trends of the Southeast (Seager 2009.) Most troublesome in this case would be Southern Florida as it is most assuredly underrepresented as will be seen in chapter 2.

Liang et al. (2006) presented an example of this. The global model used in the study underestimated the previously mentioned "warming hole" in the South-Central United states by up to 1.5° for a summer climate. The reasoning here is that the regional model used a physics package that was more consistent with the physics of the region being modeled. In this case, the conditions proposed by Pan et al. (2004) for obtaining a warming hole were present in the regional model, and not the global model.

1.5 – Objectives and Outlines

The objective of this study is to understand the model projections of the summer season climate over the Southeastern United States in the late 21st century. To do this, we will analyze the global model results and also examine the regionally downscaled results from a regional model. Chapter 2 will look at the model and observation data used, providing a short description of each. The models discussed are the CCSM3 and the RSM and sections for both contain a brief summary of model physics. NCEP Stage IV precipitation data are also discussed in brief. Chapter 3 covers the results obtained during the study as well as brief explanations of the methodologies employed. Chapter 4 offers a brief summary of the results and proposes future work to be done.

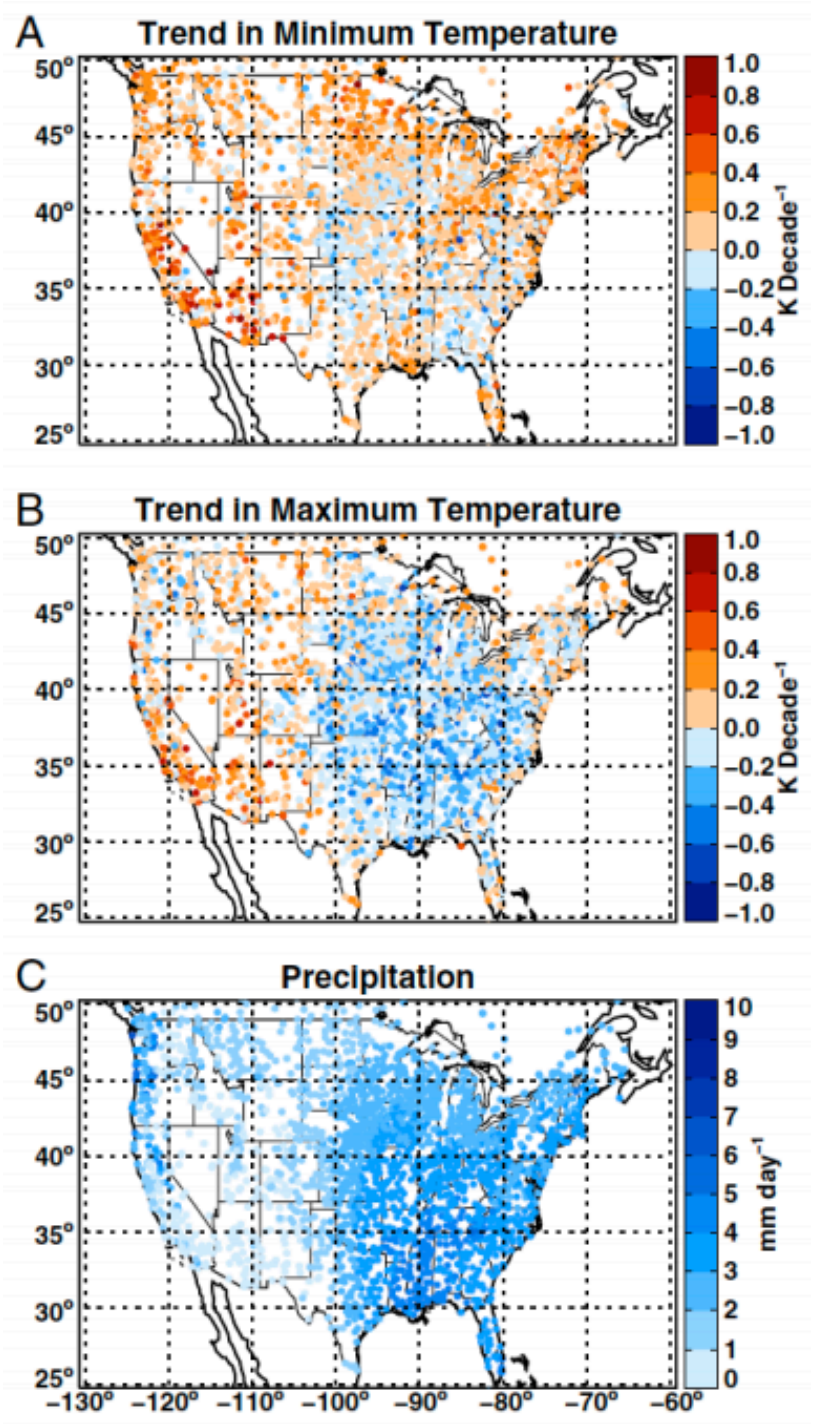

Fig. 1.1. (From Portmann et al. 2009, their Fig. 1) Maps of 1950-2006. (A) Minimum temperature trends for May-June, (B) same as A but for the maximum temperature, and (C) mean daily precipitation (mm/day) but for March-June time period (earlier months included because effects if precipitation may persist for several months; see Discussion). All stations are shown that satisfy minimum data requirements discussed in the text.

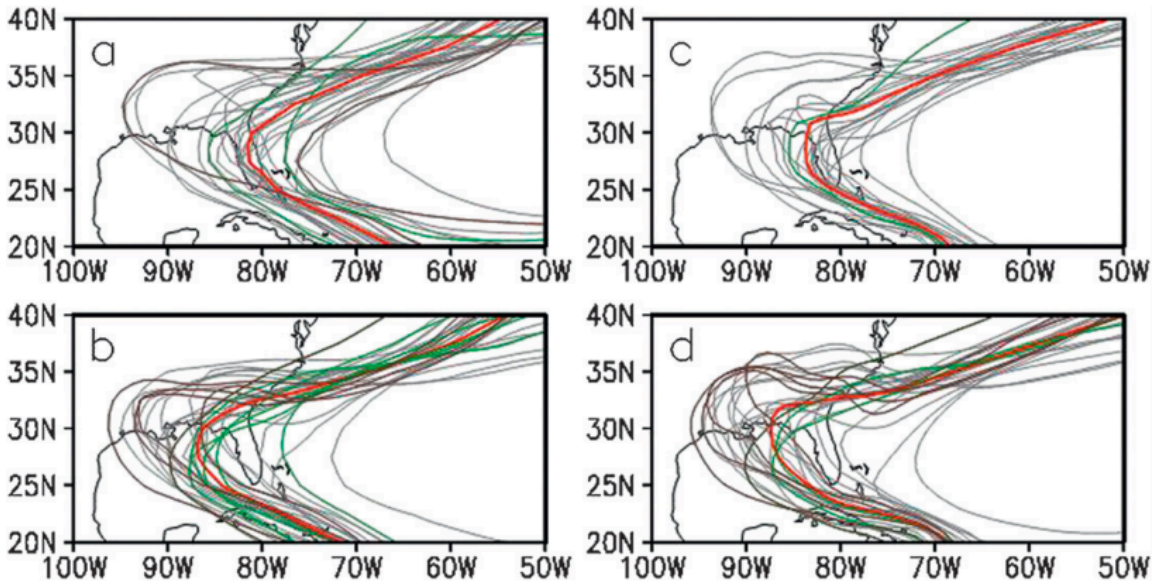

Fig. 1.2. (From Let al. 2011, their Fig. 2) Interannual variations of 1560-gpm contour line at 850 hPa during JJA in both NCEP and ERA-40 reanalysis data for the two periods considered. (a) NCEP first period 1948–77; (b) NCEP second period 1978–2007; (c) ERA-40 first period 1958–77; and (d) ERA-40 second period 1978–2002. Red thick curves represent the mean location of the NASH in JJA for the two periods, and green and brown lines represent the NASH in wet and dry years, respectively. Note ERA-40 only covers the period 1958–2002, thus the two periods considered are 1958–77 and 1978–2002 to be in agreement with the two periods considered for the NCEP reanalysis data.

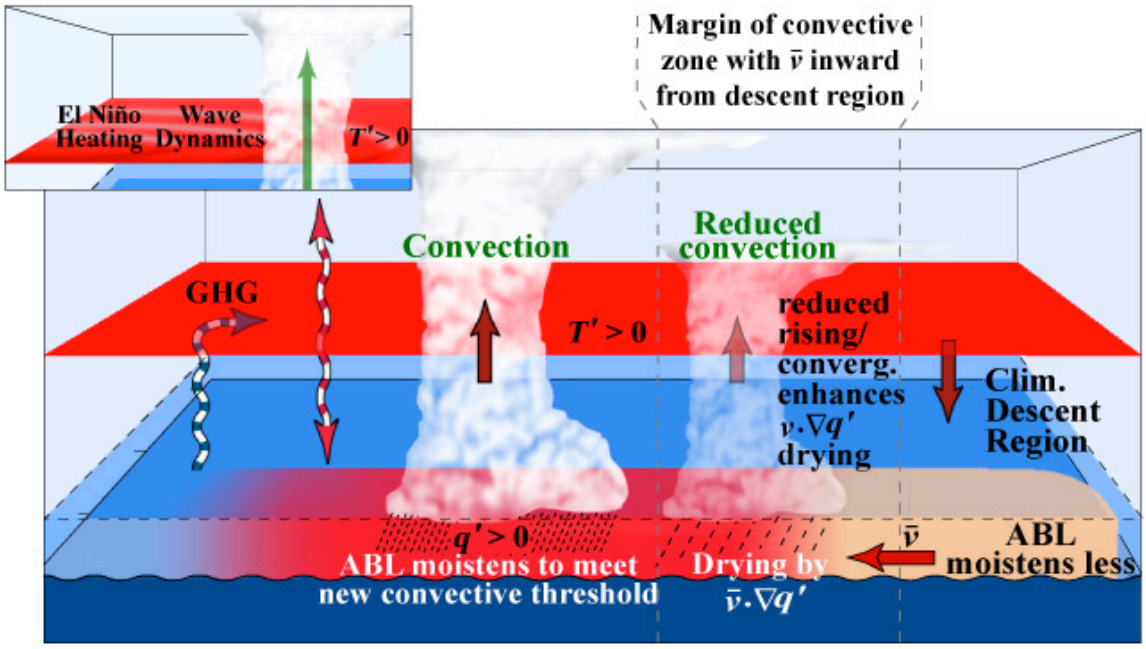

Fig. 1.3. (From Neelin et al. 2003, their Fig. 3) Schematic of the "upped-ante" mechanism for negative precipitation anomalies. For the global warming case, the tropospheric temperature warms due to increased absorption of infrared radiation (dashed curves) by greenhouse gases (GHG). For the El Nino case (inset) warming is spread from the Pacific by wave dynamics. The rest of the pathway via convective interactions is common to both. Adjustment of atmospheric boundary layer (ABL) moisture in convective regions m to meet the new convective "ante", established a gradient of ABL moisture anomalies q' relative to nonconvective regions. This creates a drying tendency where low-level flow **v** moves into the margin of a convective zone. Feedbacks reducing upward motion and low-level convergence enhance this drying tendency.

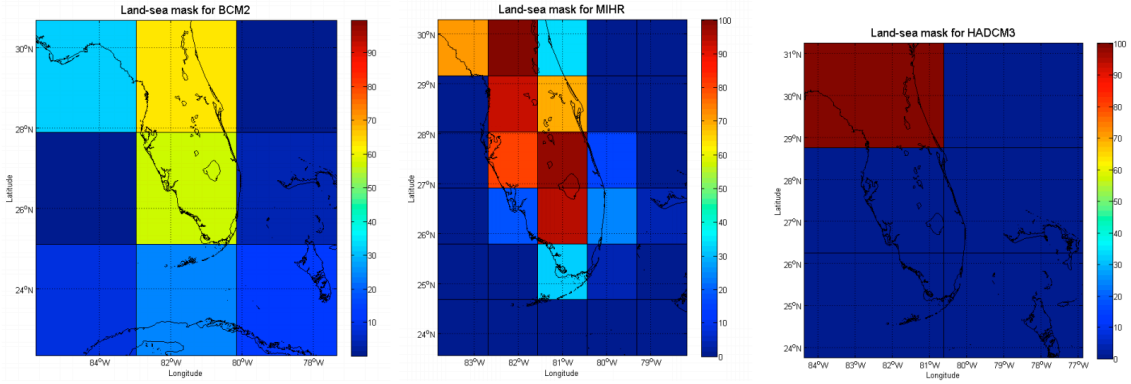

Fig. 1.4. (From Misra et al. 2011, their Fig. 6.1) The land-sea mask of three climate models (left: BCM2, middle: MIHR, and right: HADCM3) that contributed to the IPCC AR4. The deep blue color represents the ocean, and the rest of the colors represent the vegetation mask of the terrestrial surface.

CHAPTER TWO

DATA

The model output used in this study used in this study was forced with the A2 climate scenario (Nakicenoc et al. 2000). Climate scenarios are used to specify carbon dioxide concentrations in the model. Adjustments to the concentration of carbon dioxide dictate the external forcing in the model. The carbon dioxide concentration assumed by the A2 climate scenario for our future projection is roughly doubled from present-day concentrations of 350 ppm to 750 ppm, and represents the worst-case outcome. Driving this projected increase in the A2 scenario is a continued focus on non-environmentally sound technology, rapid population growth to 15 billion people, and nations that act in their personal interest. Other climate scenarios are generally more conservative in their carbon dioxide estimates as seen in Fig. 2.1.

2.1 – CCSM3

The Community Climate System Model version 3 (CCSM3) (Collins 2006) is the global climate model used in this study. The CCSM3 is a coupled climate model encompassing the atmosphere, ocean, sea ice, and land surface, all of which are linked via a flux coupler that exchanges flux and state information between components. Table 2.1 shows each of the component models used in CCSM3. The atmospheric model used by CCSM3 is the Community Atmospheric Model version 3 (CAM3). The CAM3 is based on an Eulerian spectral dynamical core (semi-Lagrangian for q). It employs a macroscale parameterization of evaporation and condensation to describe temperature changes between phase changes, and a microscale parameterization for the conversion of condensate to precipitate (Collins 2004). The model does not treat land, sea, and ice surfaces discretely as in earlier climate models. Originally, grid cells within the model were treated as being either wholly land or wholly sea. In CAM3, a grid cell can be treated instead as 50% land and 50% sea. A very important facet of the CAM3 lies in its ability to model regions of multiple cloud overlap, improving calculation of radiative fluxes. Aerosols are treated non-uniformly in CAM3 simulations. Finally, evaporation of precipitation

from convection is more consistent over previous versions, allowing the CAM3 to offset any drying by modification of longwave radiation.

The CCSM has a horizontal resolution of 1.4° by 1.4° with 26 vertical levels. Model output is at a six-hourly interval, and covers the periods 1969 to 1999 and 2040 to 2070. Owing to its coarse resolution, the CCSM3 is generally well suited for diagnosing changes in large-scale features like the NASH. The land/sea mask as well as topography is plotted for our region in Fig. 2.2.

2.2 – RSM

The regional model used for this study is the Regional Spectral Model (RSM) (Juang and Kanamitsu 1994; Kanamitsu et al. 2002), forced with CCSM3 output at the lateral boundaries. Model physics and characteristics are described in Table 2.2. This model differs from the CCSM3 explained above, as it is a dynamically downscaled, regional model. The RSM offers an increase in spatial resolution over the CCSM3, thereby resolving Florida's landmass and coastlines as well as the topography of the Appalachian Mountains (Fig. 2.3). Likewise, it offers a better view of the Southeast's vegetation (Fig. 2.4).

The RSM uses output from the CCSM3 to feed the lateral boundary conditions every six hours (Misra et al. 2011). To offset any large-scale errors in the RSM output that result from the downscaling process, a scale-selective bias correction scheme (Kanamaru and Kanamitsu 2007) is applied. This method allows the interior of the model to be relatively insensitive to its boundaries. As a result, the downscaled output is less dependent on the domain size. Furthermore, applying a scale-selective bias correction scheme reduces the model's dry biases in summer precipitation (Kanamaru and Kanamitsu 2007).

Another strength of the RSM lies in its ability to properly depict the time of maximum precipitation in the Southeast (Stefanova et al. 2011). Figure 2.5 (adapted from Stefanova et al. 2011, their Figure 13) shows the RSM timing of maximum precipitation when the RSM is forced with NCEP-R2 reanalysis data. The RSM produces a pattern similar to the pattern seen in NCEP/EMC observed rainfall data. When the RSM is forced with CCSM3 output, the result does not change significantly (Fig. 2.6). In contrast, the CCSM2 poorly depicts the time of maximum precipitation

by about 6-10 hours, as seen in Fig 2.7 (Dai 2006, his Fig. 17). The CCSM2 timing of maximum rainfall is noted to not be significantly different from the timing of maximum rainfall in CCSM3.

2.3 – Observed Data

The rainfall observations used in this study come from NCEP Stage IV hourly precipitation analyses of the contiguous United States (Lin and Mitchell 2005). Rainfall totals, collected by multisensor analysis from National Weather Service River Forecast Centers (NWS RFC) are mapped onto a Hydrologic Rainfall Analysis Project (HRAP) grid (Greene and Hudlow 1982). If the HRAP grid cell overlaps a report from the RFC, the reported value is used; otherwise an average of nearby reports is taken. The hourly data used in this study span the period from 2002 to 2010. All of 2007 is excluded from this data set due to missing data.

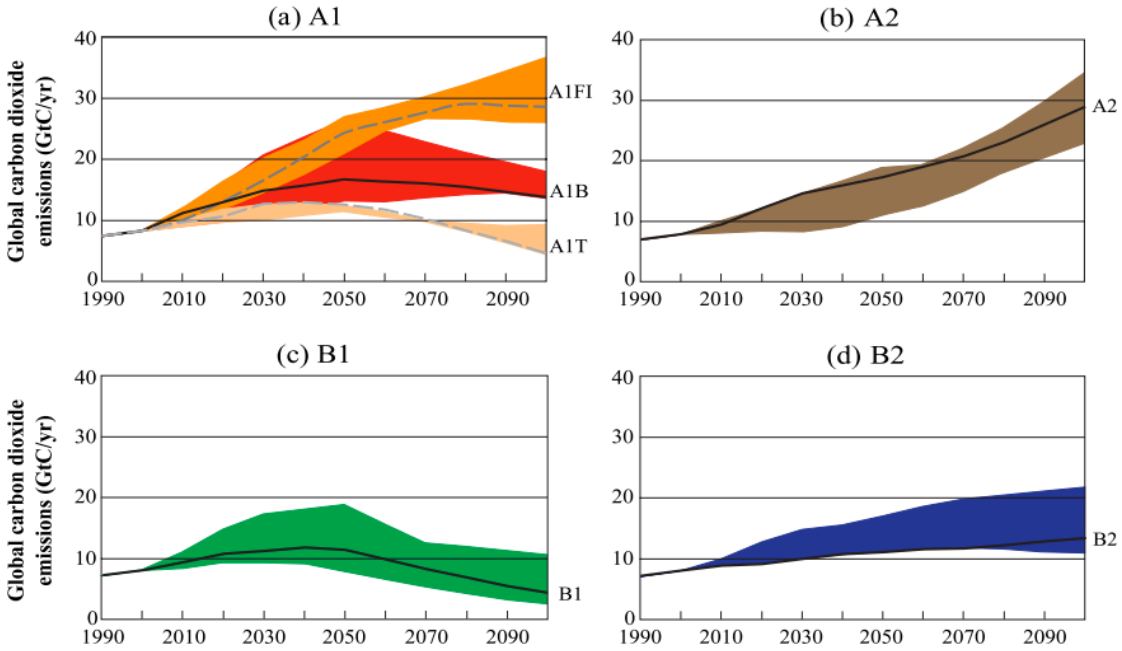

Fig. 2.1. From the IPCC Special Report on Emissions Scenarios (2000), showing projected changes in global carbon dioxide emissions under the A1, A2, B1, and B2 scenarios.

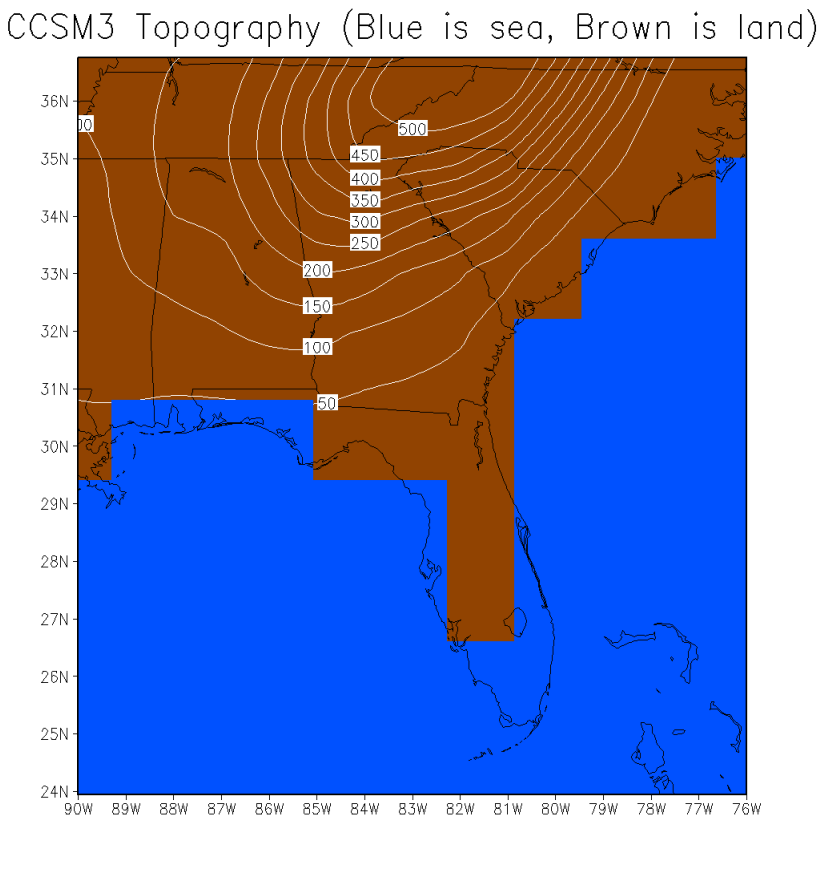

Fig. 2.2. CCSM3 topography (contoured) and land/sea mask. Brown is land, blue is sea.

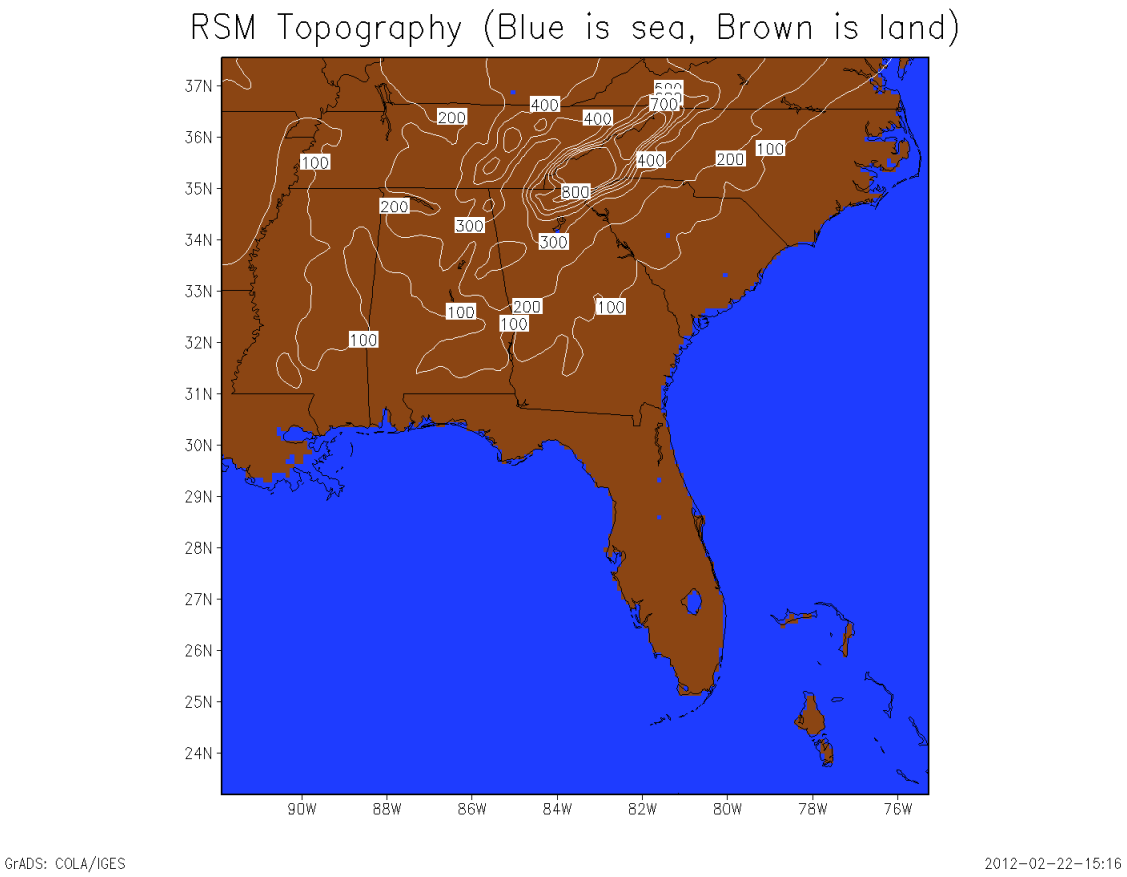

Fig. 2.3. RSM topography (contoured) and land/sea mask. Brown is land, blue is sea.

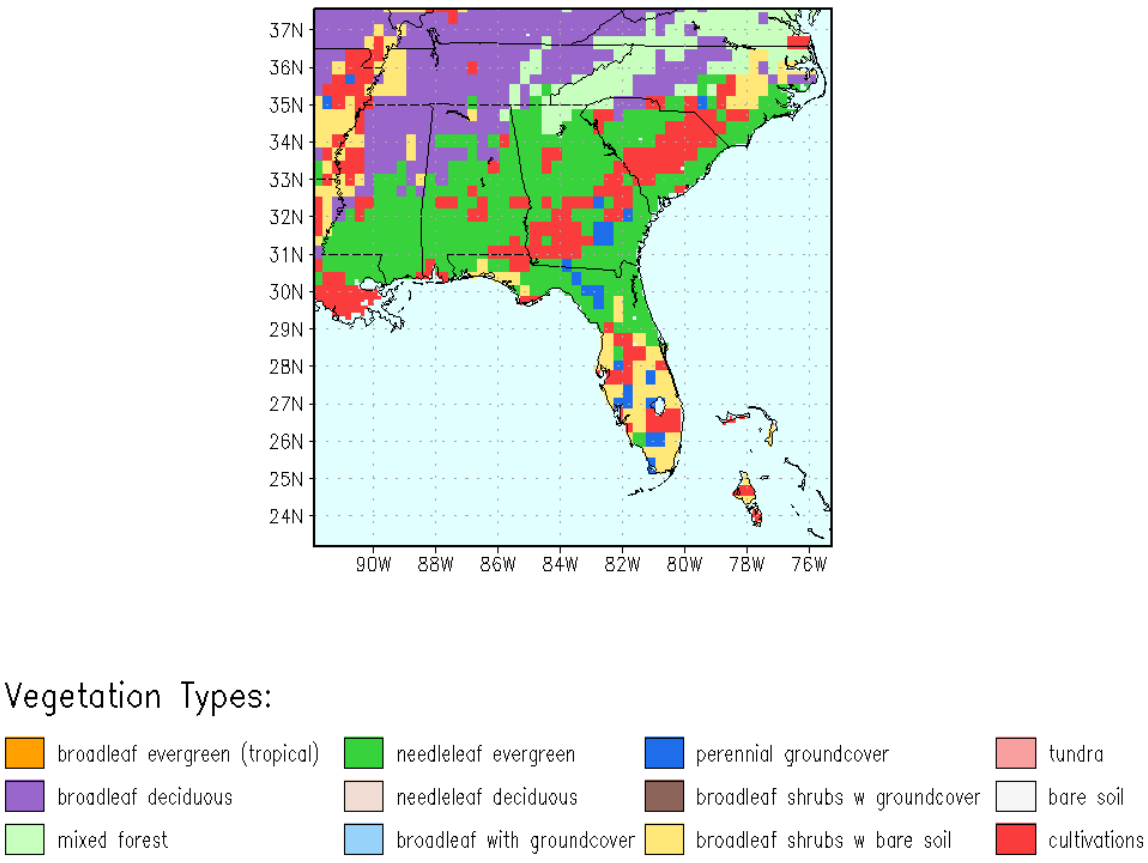

Fig. 2.4. Vegetation map used by RSM.

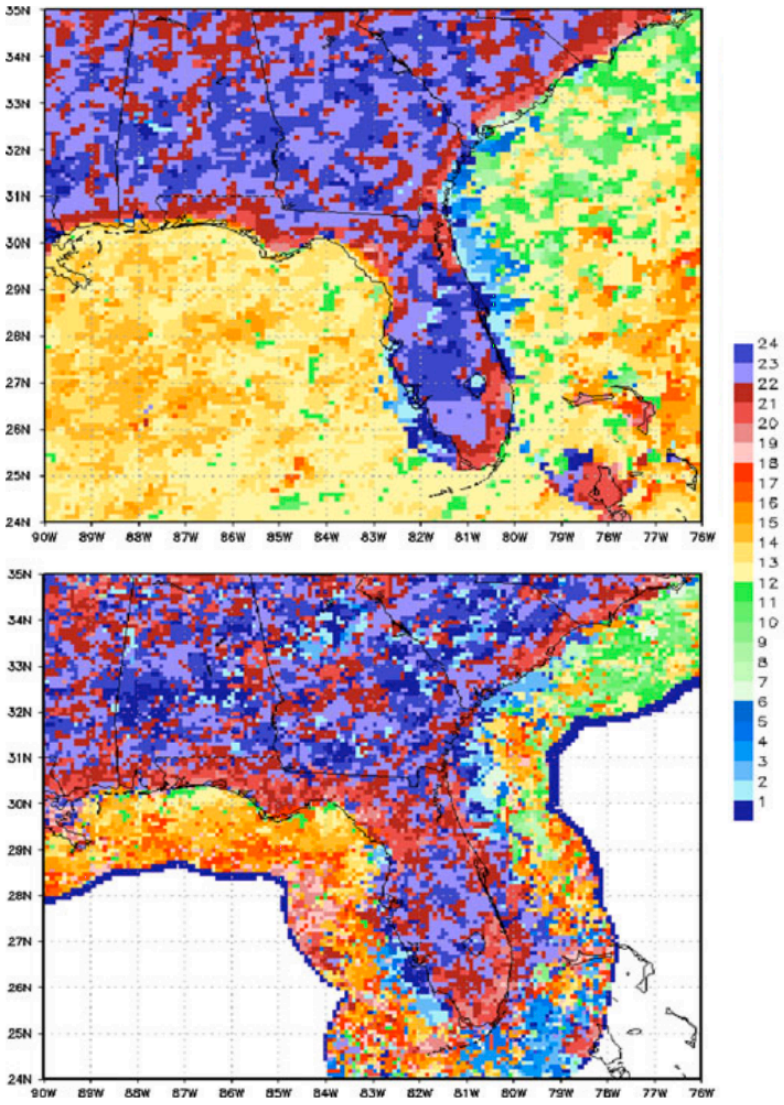

Fig. 2.5. (From Stefanova et al. 2011, their Fig. 13) Average timing of the 1979-2001 JJA diurnal maximum [of rainfall] between CLARReS10-R2 (top) and the average timing of JJA diurnal maximum [of rainfall] from NCEP/EMC multi-sensor estimate for 2004-2009 (bottom).

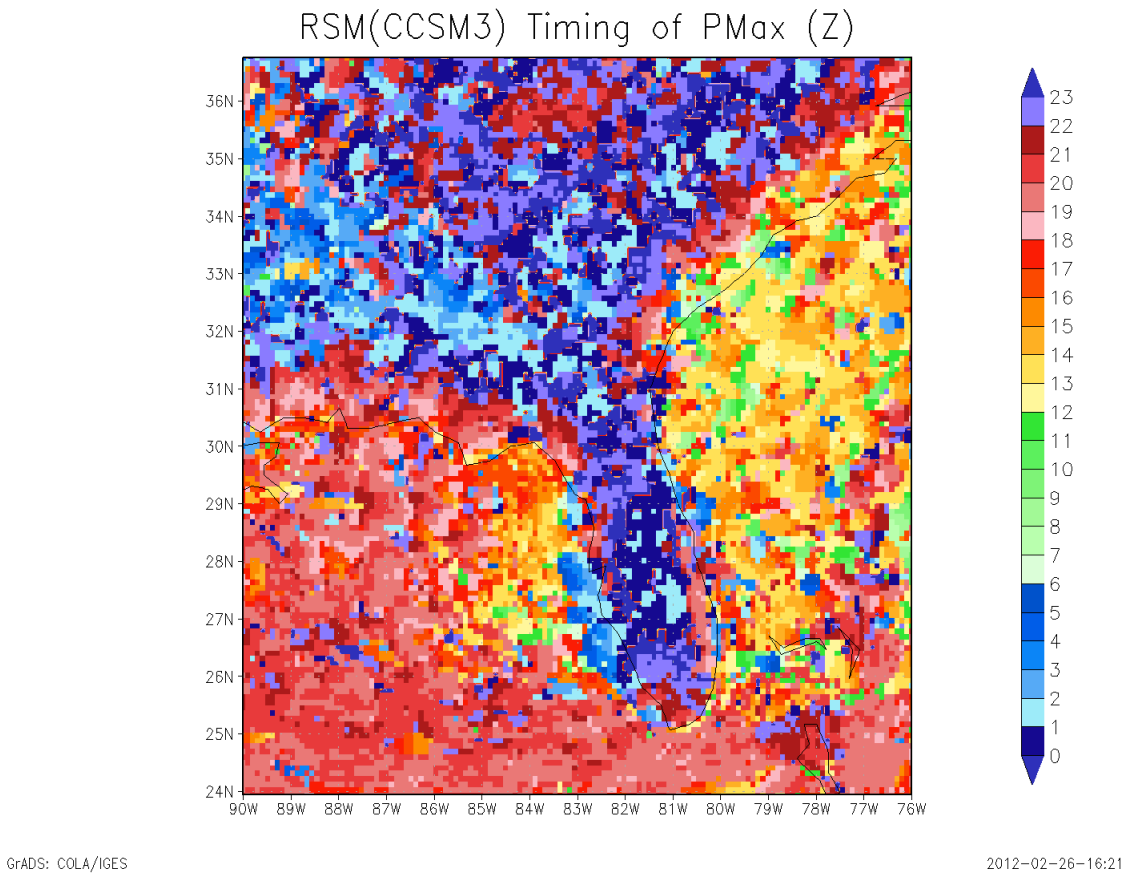

Fig. 2.6. Same as Fig. 2.4 but for RSM forced with CCSM3 model data for 1969 to 1999.

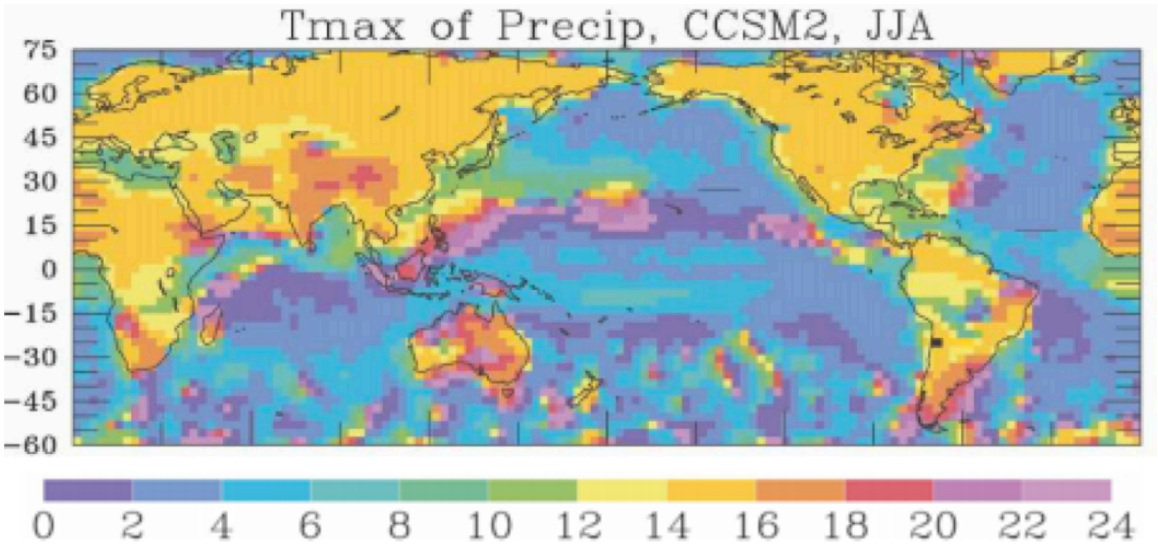

Fig. 2.7. (Adapted from Dai 2006, his Fig. 17) Timing of maximum precipitation for the CCSM2. Dai (2006) stated that CCSM2 results are nearly identical to CCSM3.

Table 2.1 – Summary of component models used in the CCSM3.

Domain	Model
Atmosphere	Community Atmosphere Model version 3 (CAM3; (Collins et al. 2004, 2006a)
Ocean	Parallel Ocean Program version 1.4.3 (POP; Smith and Gent 2002)
Land	Community Land Surface Model version 3 (CLM3; Oleson et al. 2004; Dickinson et al. 2006)
Sea ice	Community Sea Ice Model version 5 (CSIM5; Briegleb et al. 2004)

Table 2.2 – Breakdown of the Regional Spectral Model

Model	Description
Domain	23.181°N to 37.543°N, and 75.264°W to 91.878°W.
H. resolution	10 km horizontal
V. resolution	28 vertical sigma levels
Topography	30 minute USGS
Vegetation map	USGS vegetation converted to 12 NOAH types (Loveland et al. 1995)
Land surface scheme	NOAH w/4 soil levels (Ek et al. 2003)
PBL scheme	Nonlocal (Hong and Pan, 1996)
Radiation scheme	(Chou and Lee 1996; Chou and Suarez 1994)
Convection scheme	Simplified Arakawa Schubert scheme (H.-L pan and W.-S. Wu 1995)
Cloud water scheme	Diagnosed from relative humidity (Slingo 1987)

CHAPTER THREE

RESULTS & METHODOLOGY

3.1 – Outline of Process

In this study, we examined how a global climate model's projection of precipitation over the Southeast in the late 21st century differs from a regional model's projection. To do this, we first calculated summer seasonal mean rainfall for both models over the two previously mentioned time periods. We found a disparity in the projections; the global climate model projected a dipole pattern in rainfall, while the regional climate model projected a universal drying of the region. This disparity is explained by determining at the impact of diurnal variance of rainfall on seasonal variance of rainfall. We then used physical mechanisms to further explain the disparity in projections. The first is the "upped-ante" mechanism, which is diagnosed through tropical SSTs and tropospheric temperature projections in the late 21st century. The second physical mechanism we look at is the expansion of the NASH. Finally, we questioned if the models project a stabilization of the atmosphere in the late 21st century by looking at how precipitable water, and surface lifted index are projected to change in the models.

3.2 – Confirming the Reduction in Diurnal Variability

We first examine CCSM3 projections for precipitation in the Southeast in the late 21st century. We accomplish this by calculating a seasonal mean precipitation in both the 20th and 21st centuries and computing a difference in rainfall of the two periods. Figure 3.1 shows the mean seasonal precipitation plots, the bottom showing the difference in rainfall between the two time periods. We see that the CCSM3 projects a dipole pattern in precipitation across the Southeast. The RSM, on the other hand, depicts a different pattern. Figure 3.2 shows analysis similar to that of Fig. 3.1, but for the RSM. We see an overall drying of the Southeast in the late 21st century when using the RSM. In order to understand why the patterns are different, we looked at each model's ability to resolve the diurnal variability of precipitation.

The diurnal fraction of variance of summer seasonal precipitation is calculated for observations and the RSM. This is accomplished by calculating a mean

for seasonal daily precipitation and a mean value for the diurnal amplitude of rainfall. The variances of seasonal daily precipitation and diurnal amplitude of rainfall are then calculated using these values, and each respective variance is averaged for the period. A ratio of the diurnal precipitation variance to the seasonal daily precipitation variance is then calculated and plotted (Figs. 3.3 and 3.4). This method is performed for the observation data from 2002 to 2010 (excluding 2007) as well as the model data for the late 20th and 21st centuries. These calculations are not done for the CCSM3, as the outputted data are available only at a six-hourly interval, far too coarse to diagnose a diurnal range. These ratios are calculated to determine if a reduction in diurnal variability of precipitation would produce a significant effect on mean seasonal precipitation. Calculations from the RSM (Fig. 3.3) show that in the 20th century diurnal variability in precipitation can account for 15 to 20 percent of total fractional variance of seasonal precipitation. In the 21st century the RSM continues to show that diurnal variability explains a large portion of the variance of JJA seasonal precipitation. Figure 3.4 shows a similar analysis for the observational data. From observations, we see that diurnal variance of precipitation accounts for 20-40% of the total seasonal variance in precipitation. The diurnal fraction of variance is somewhat smaller in the model (generally by around 10 percentage points) than in the observations. However, the observed variance is computed over an 8-year period, in contrast to the 23-year period from the RSM. Expanding the calculation of observed variance to a 23-year period might bring the RSM and observed results closer together. Regardless, the RSM is seen to underemphasize the contribution of diurnal fraction variance of JJA mean precipitation.

We cannot perform the same analysis for CCSM3, however we can conceptually analyze its ability to resolve diurnal variation. The CCSM3 very likely incorrectly depicts the diurnal variability of precipitation, again, owing to its poor topography and land/sea masking as well as its poor timing of maximum precipitation. Given that all of these characteristics are involved in some way with precipitation (as noted in the introduction), incorrectly modeling any of the characteristics will enhance uncertainty in the confidence of a projection.

Interestingly, the seasonal rainfall pattern projected by the CCSM3 is not inconsistent with other global climate models, as seen in figures adapted from NARCCAP (Fig.3.5). The two models, CGCM3 and GFDL both show a similar dipole pattern in seasonal rainfall across the Southeast. Other models, not depicted here, demonstrate a similar pattern to CCSM3, as well.

Taking the above facts into consideration, there is some evidence that the projection by the RSM is more plausible than the projection of CCSM3. The key characteristic is that the RSM is likely resolving afternoon thunderstorms. Afternoon thunderstorms are the prime driver of diurnal variability in the Southeast. The timing of maximum rainfall in the RSM bolsters the fact that afternoon thunderstorms are being resolved. Typically, in the Southeast, afternoon thunderstorms occur in the early-evening hours, and produce the heaviest rainfalls for the day. Resolution of these storms, then, would be key for making reliable seasonal predictions in rainfall. Given that the RSM resolves at least some portions of afternoon thunderstorms, the RSM allows for a more plausible diagnosis of precipitation projections in our study. Because of this reliability, we look at the RSM projection of daily maximum and minimum rainfall to assess if the overall drying is symptomatic of a reduction in the diurnal range of precipitation. To do this, we first need to filter out any synoptic scale influences on the regions. We do this by calculating a 31-year mean precipitation at the climatological time of maximum and minimum precipitation. This technique is applied for both time periods, and the analysis is plotted (Fig. 3.6). This figure shows that the diurnal range of precipitation is reduced in the 21st century, and a majority of the reduction occurs in the maximum values of precipitation. The synthesis of Fig. 3.2 and Fig. 3.6 ultimately prove that there is a regional drying of the Southeast through modulation of the diurnal variability of precipitation in the late 21st century (according to the RSM.)

3.3 – Physical Mechanisms Behind the Drying

With the differences between the two model projections identified we now discuss possible explanations for why any changes in precipitation are seen. First, we determine if the “upped-ante” effect is appearing in our region. To do this, we look at tropospheric temperatures, as they are noted to be the impetus of the

"upped-ante" effect. However, we should first identify a cause within the models for tropospheric temperatures to increase. We analyze seasonal mean sea surface temperatures (SST) in the CCSM3 (Fig. 3.7) and see an almost universal increase in SST in the 21st century, excepting a few regions near Antarctica. Warming of tropical SST in particular is strongly correlated with warming of tropospheric temperatures (Chiang and Sobel 2002). Therefore, we expect to see an increase in tropospheric temperatures.

Recall that under the "upped-ante" scheme, warming tropospheric temperatures under increased greenhouse gas concentrations would increase the amount of moist static energy, and by extension atmospheric boundary layer moisture, required to initiate convection. To see if tropospheric temperatures are warming we use output from the RSM to calculate tropospheric temperature anomalies of the 21st century over the Southeast. This is done by taking a weighted mean of temperatures from 850 hPa to 200 hPa and taking the difference between the 21st and 20th centuries as our anomaly. Figure 3.8 shows the results of this analysis, and as expected we see a warming of tropospheric temperature anomalies above the Southeast. As a result, at least conceptually, we should expect to see a moistening of the tropical oceans stemming from their abundance of moisture and higher tropospheric temperatures. We use conceptually here to note that not all aspects of the "upped-ante" mechanism are plotted in our analysis due to the limitations of our model domain. We would also expect to see a drying of areas lying on those convective margins due to their inability to meet the convective "ante," which does include the Southeast. The "upped-ante" effect, then, plausibly accounts for a portion of the drying seen, though the magnitude is not determined. We should also consider other potential sources of drying, however, because it would be baseless to say that the "upped-ante" mechanism is the sole dictator of rainfall decrease, especially in the CCSM3 which only projects drying over peninsular Florida. To further investigate CCSM3's rainfall projection, we investigate the model's projection of the NASH.

We then determine if CCSM3 projections include a further expansion of the NASH. To do this we calculate the seasonal mean sea level pressure (MSLP) for the

Atlantic Basin for both time periods. We then plot the difference, which is seen in Fig. 3.9. MSLP is increased by about 0.3 to 0.6 hPa over the lower half of the Southeast. Also, MSLP over the Eastern Atlantic is decreased by as much as 1 hPa. Both of these changes in pressure are consistent with previously mentioned work by Li et al. (2011) and imply that the CCSM3 does project an expansion of the NASH over the Southeast in the late 21st century. As a result of this expansion, subsidence over the Southeast is increased, enhancing atmospheric stability and accounting for additional drying over the region. This expansion of the NASH in conjunction with a highly probable influence of the "upped-ante" effect provides a plausible explanation for the drying of Florida seen in the projection of the CCSM3.

Finally, we plot the seasonal mean lifted index for the Southeast to confirm that the atmosphere is becoming more stable (Fig. 3.10). Lifted index is determined by taking the environmental temperature of the air at 500 hPa, and subtracting from it the temperature of a parcel of air at the surface raised to its lifting condensation level, then raised moist adiabatically to 500 hPa. As we see, the atmosphere does indeed become more stable in the late 21st century, particularly over peninsular Florida. Symptomatic of the increase in stability is an increase in precipitable water over the Southeast in the 21st century, as seen in Fig. 3.11. This increase in precipitable water is particularly interesting for its implication for radiative forcing in the area. Because water vapor is an exceptional absorber of longwave radiation, an increase in precipitable water can create a positive feedback loop for warming. This feedback can further exacerbate the patterns in precipitation projections.

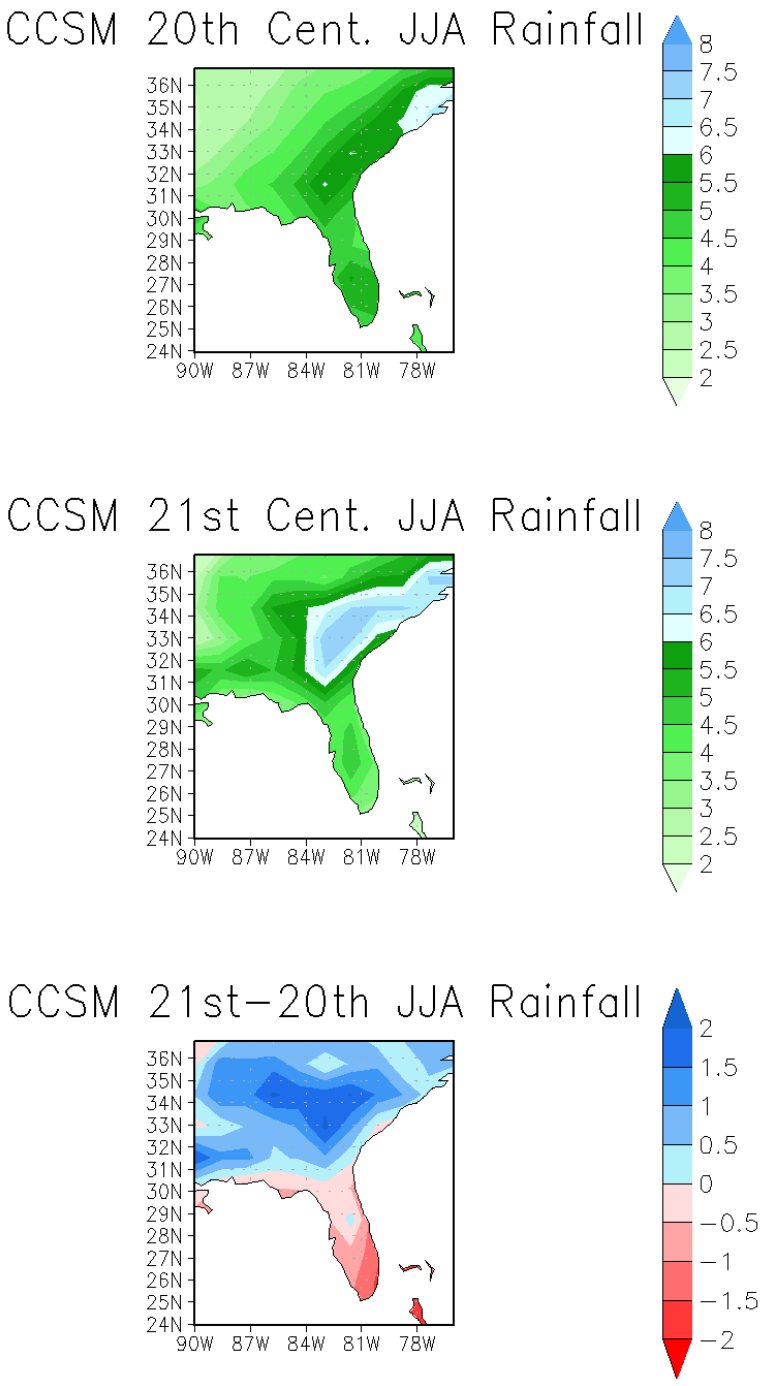

Fig. 3.1. JJA mean 31-year rainfall from the CCSM3. Units are in m/day. The top panel is for the period 1969-1999. The middle is for the period 2040-2070. The bottom panel is the difference of the two.

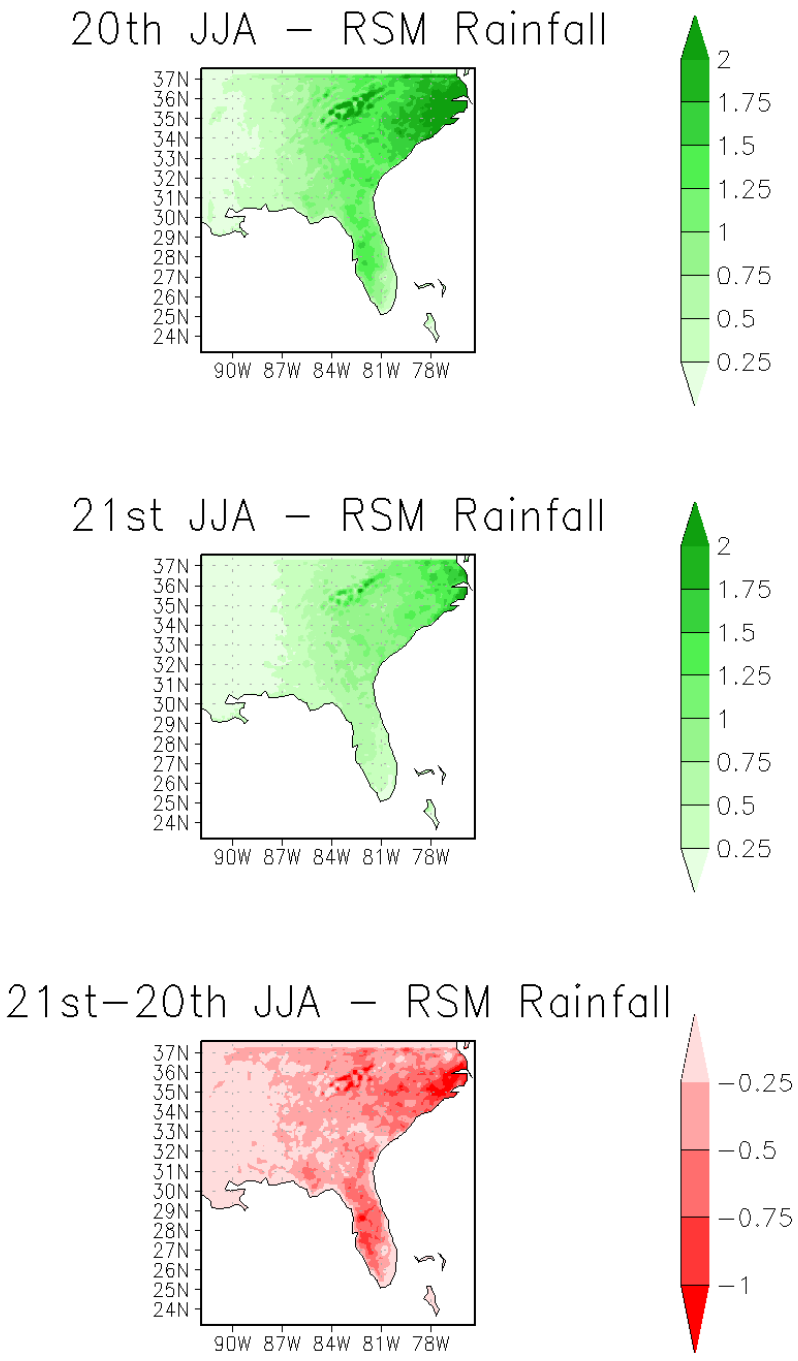

Fig. 3.2. Same as Fig. 3.1, but for the RSM. Units are in mm/day.

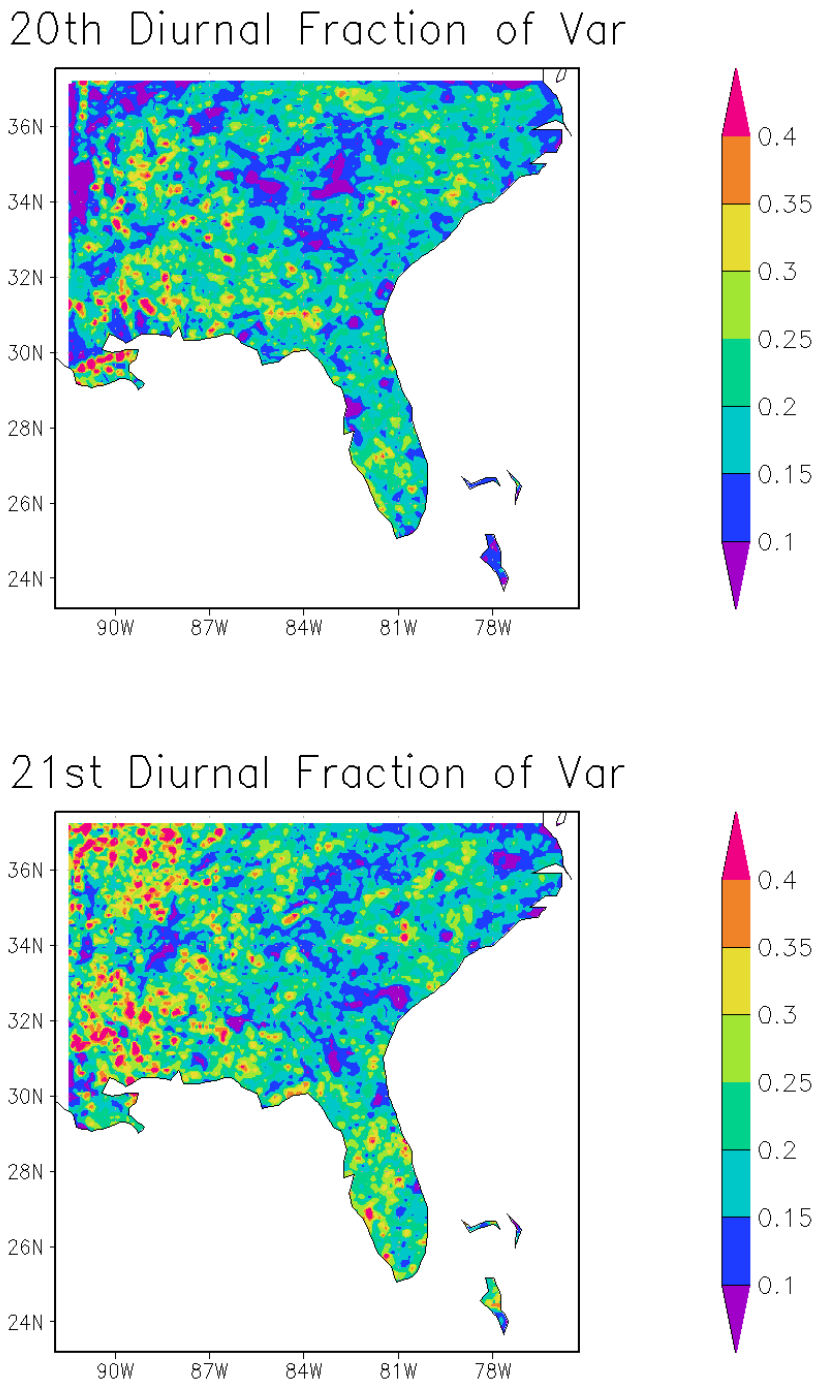

Fig. 3.3. RSM diurnal fraction of variance of total seasonal rainfall for JJA precipitation. Dimensions are fractional, and hence unitless.

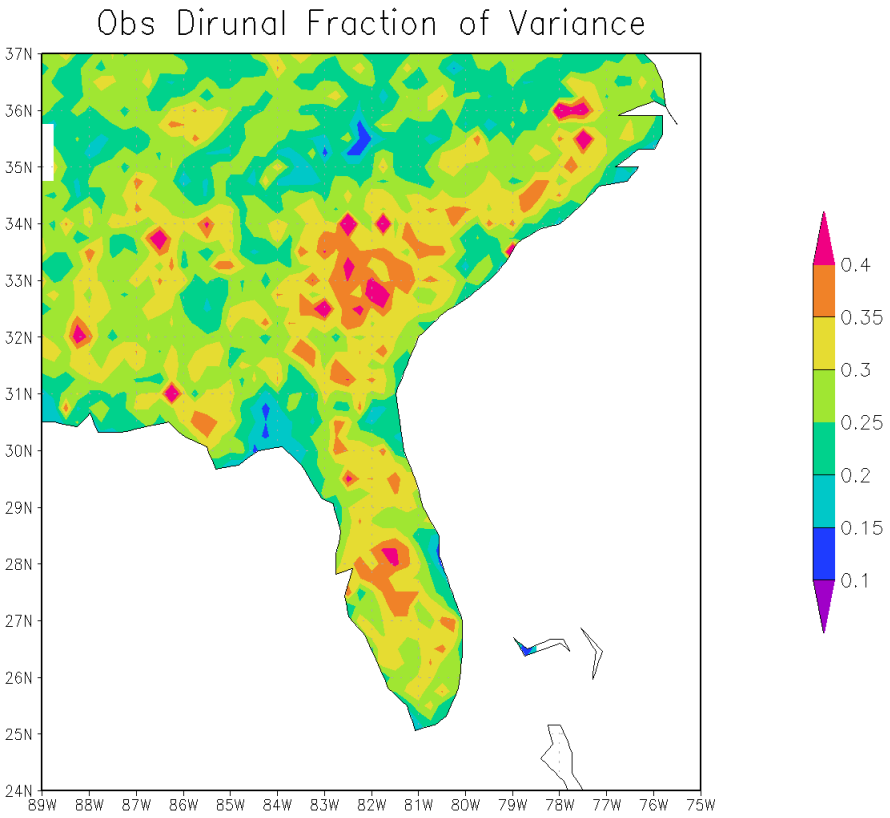

Fig. 3.4. Same as Fig. 3.4, but for the NCEP STAGE IV precipitation observations (2002-2010, excluding 2007).

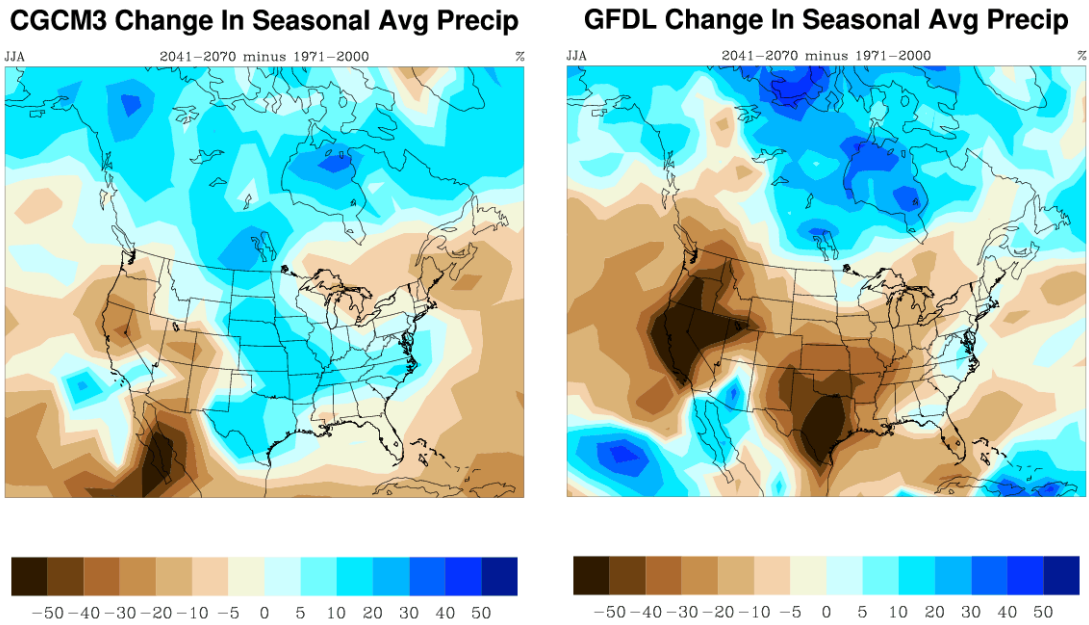

Fig. 3.5. (From NARCCAP) JJA mean rainfall from CGCM3 (left) and GFDL (right), both demonstrating a dipole pattern in precipitation. Units are in percentages.

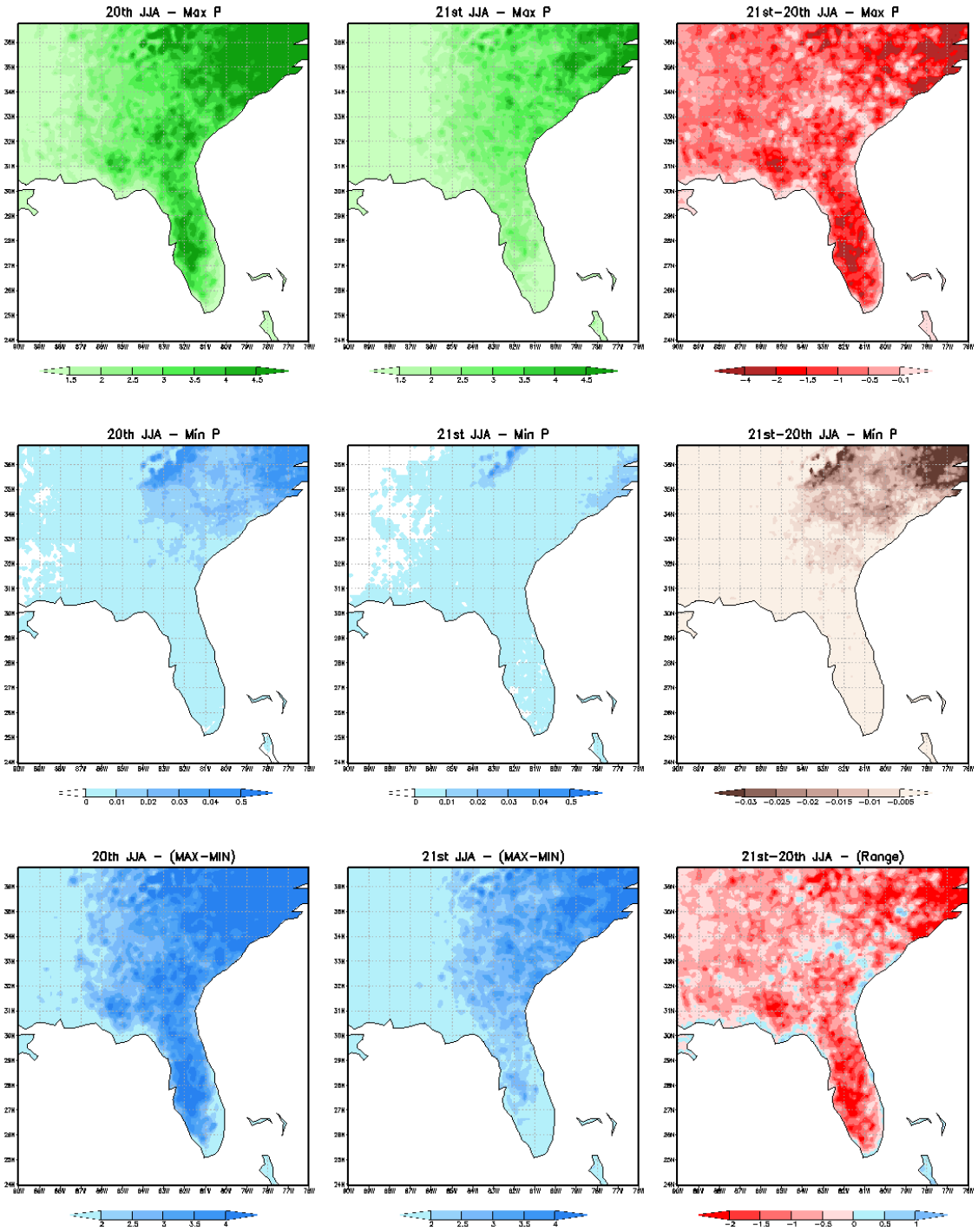

Fig 3.6. RSM diurnal range of rainfall. The top left quadrant of panels is plots of the JJA 31-year mean maximum and minimum precipitation. Each hour is averaged over the 31-year period. The plots below these show the diurnal range of precipitation (MAX-MIN). The panels on the far right show the differences between 21st and 20th century values.

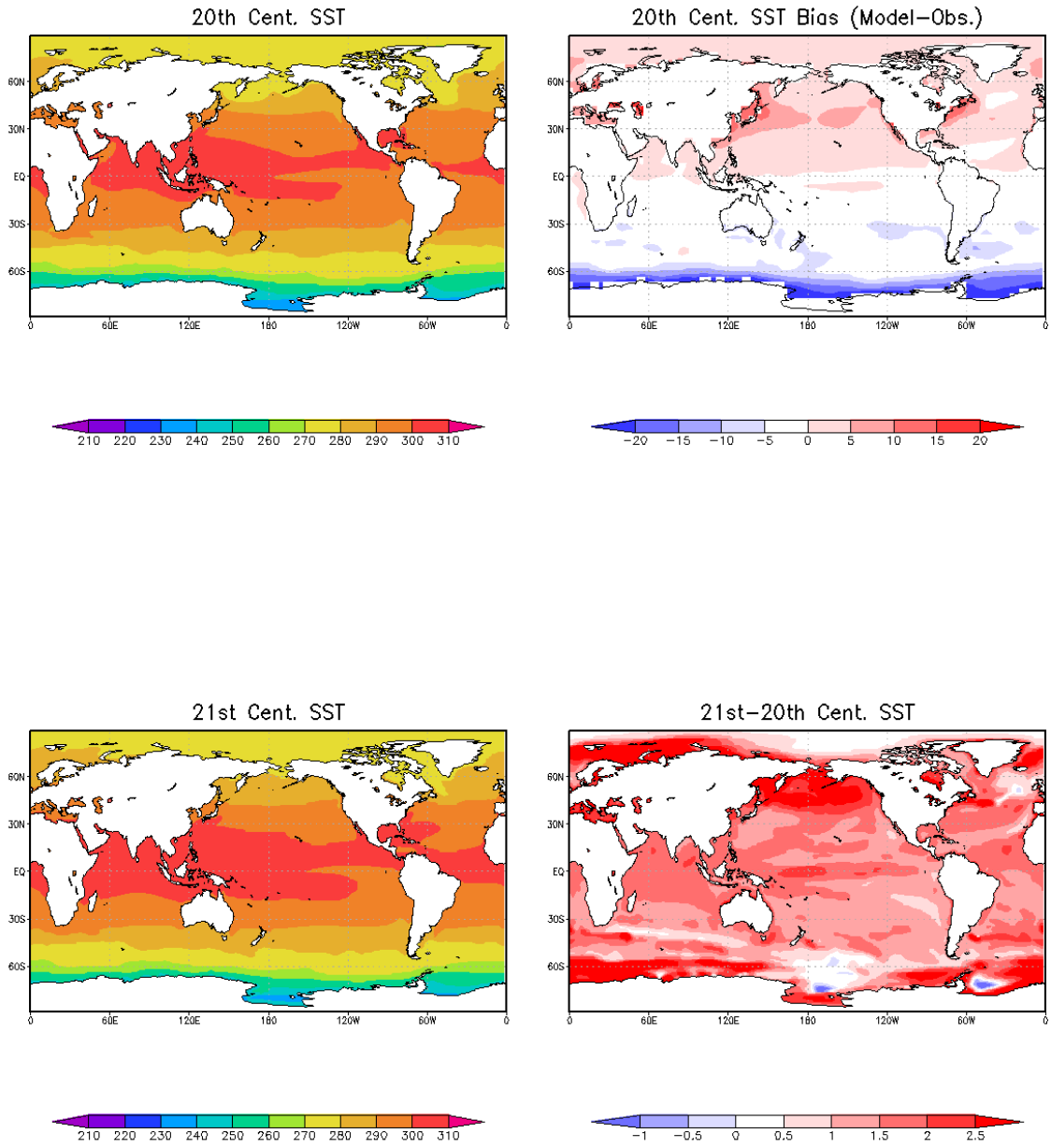

Fig. 3.7. Top left panel: 20th century JJA mean SSTs from CCSM3. Bottom right panel: Same as top left, but for 21st century. Top right panel: CCSM3 20th century difference from observed SSTs. Bottom right panel: Difference between bottom left and top left panels.

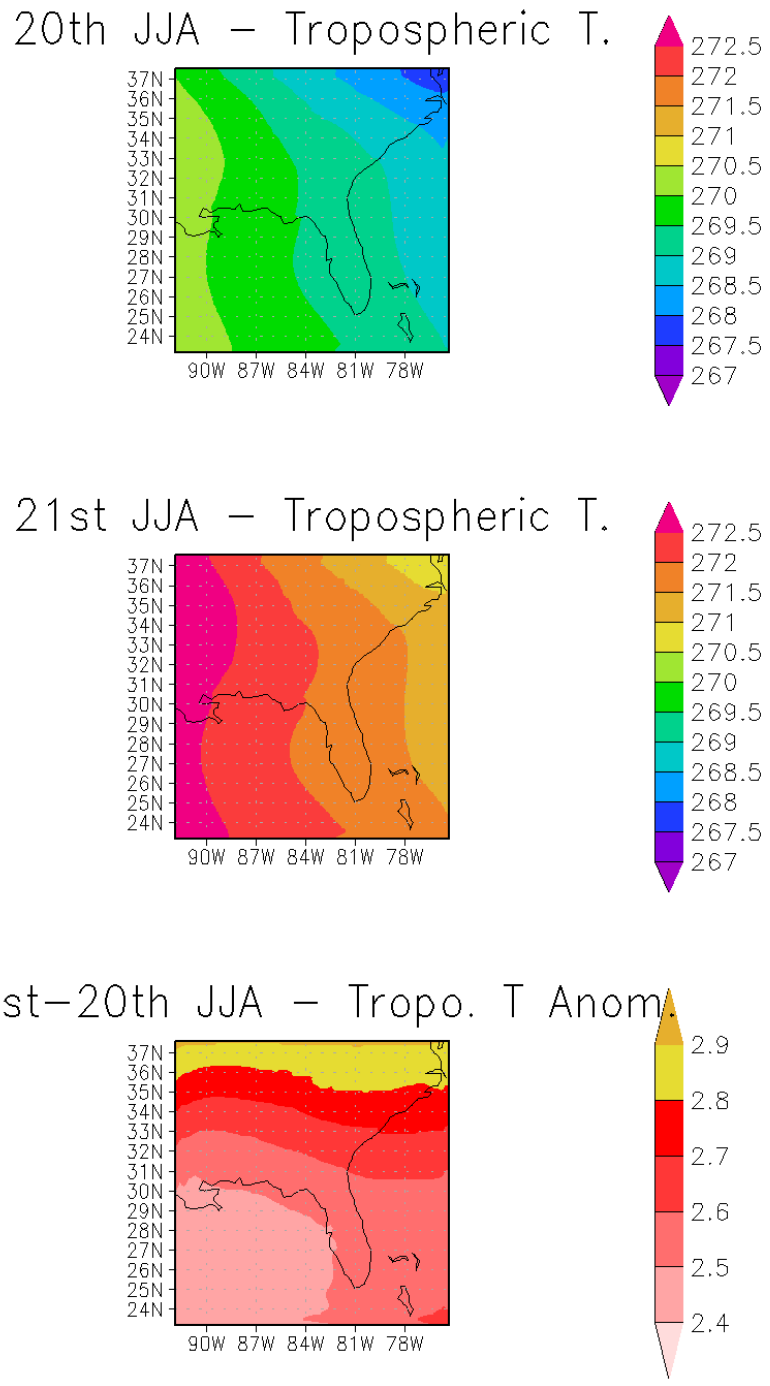

Fig 3.8. Top panel: RSM 20th century JJA mean tropospheric temperatures, with units of Kelvin. Middle panel: Same as the top, but for the 21st century. Bottom panel: Mean tropospheric temperature anomalies between 21st and 20th century. The anomaly is calculated by assuming the 20th century mean to be the mean value, and the difference from the 21st century is taken to be the anomaly.

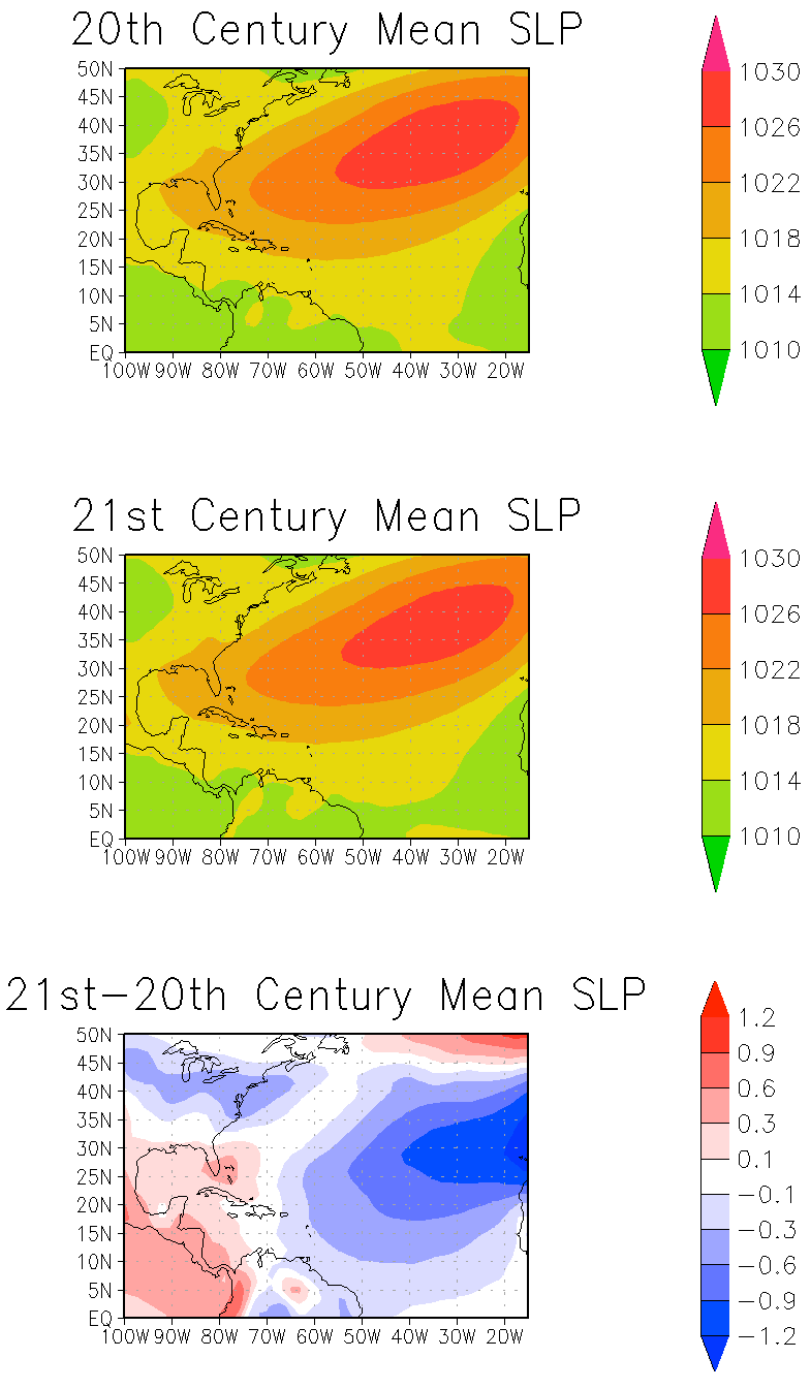

Fig 3.9. Top panel: CCSM3 20th century mean JJA sea level pressure. Middle panel: Same as the top, but for the 21st century. Bottom panel: Difference in sea level pressure between middle and top panels.

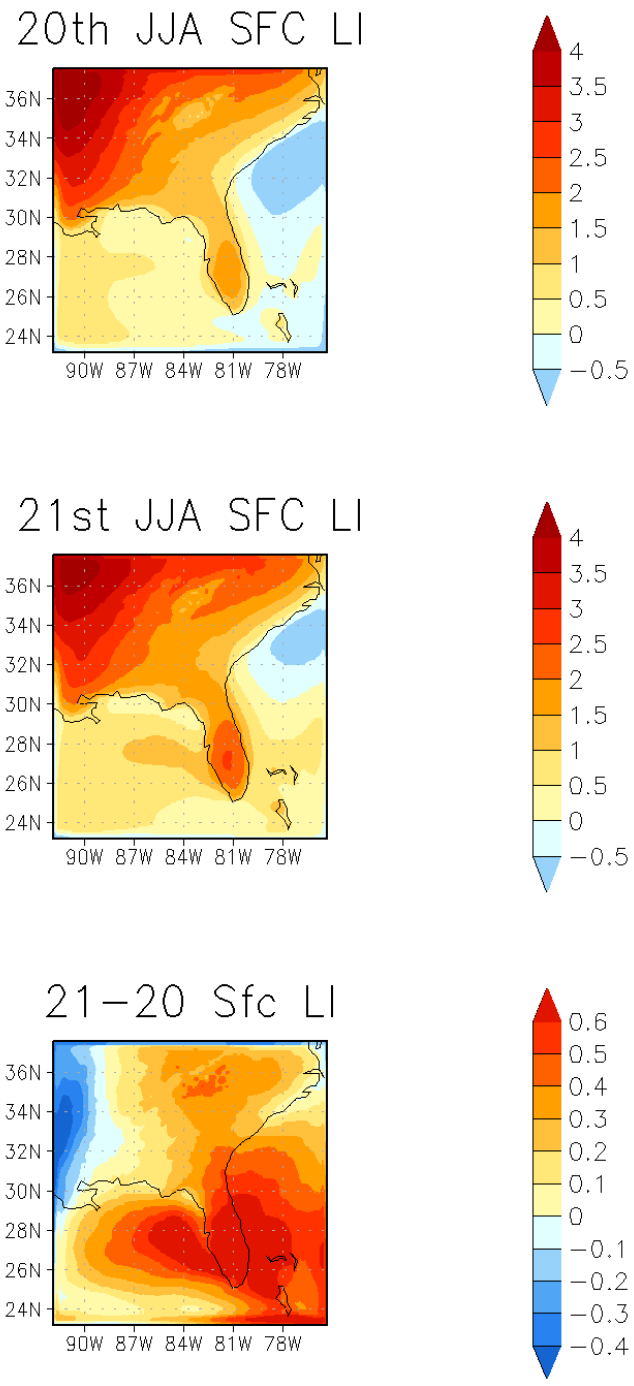

Fig. 3.10 – Same as Fig. 3.3, but for surface lifted index. Units are in K.

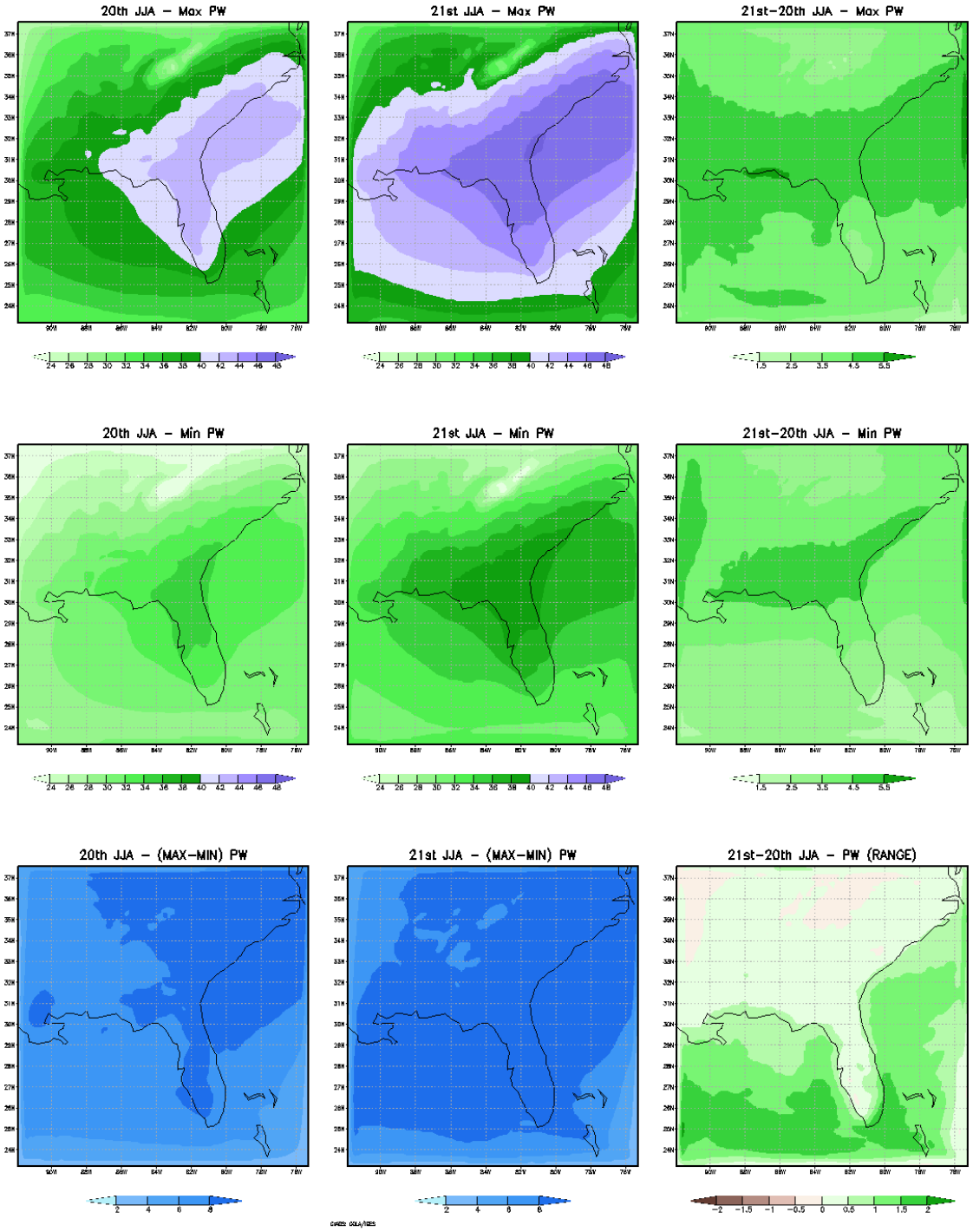

Fig 3.11 – Same as Fig. 3.6, but for RSM atmospheric columnar precipitable water. Units are in kg/m^2.

CHAPTER FOUR

CONCLUSIONS

4.1 – Conclusions

We have seen how a global climate model projection of precipitation over the Southeast in the late 21st century summer differs from projections of a regional climate model. According to calculations from observed data, diurnal variance of rainfall represents 20-40% of the seasonal mean variance of rainfall. The global climate model, which incorrectly depicts the timing of maximum rainfall, topography and coastlines, likely does not represent diurnal variability. Failing to resolve diurnal variability of rainfall in the Southeast negatively impacts the reliability of your seasonal forecast, and as such the projection offered by CCSM3, seen to a dipole, is considered to be dubious.

A dynamically downscaled, regional model that resolves the diurnal variability, on the other hand, projects a uniform drying response in precipitation in the late 21st century. This result is more plausible, though it should be noted that the RSM used in this study underestimates the significance of diurnal variance of precipitation relative to the seasonal mean variance. This trend can also be attributed to the model's more accurately represented vegetation, coastlines, topography, and timing of maximum rainfall in the region, which leads to more consistent representation of the region's physics.

Beyond diurnal variability of precipitation, this drying is likely caused by two physical mechanisms. The first of these mechanisms is the "upped-ante" mechanism of convection. In the late 21st century, the CCSM3 projects a universal warming of SST. Warmed Tropical Pacific Ocean surfaces are tightly correlated with warmed Tropical Atlantic tropospheric temperatures. As the troposphere of the Tropical Atlantic warms, the amount of moist static energy, and by extension, ABL moisture required for initiating convection increases. Though the model domain does not cover the Caribbean Sea, we can reasonably assume that the moisture "ante" required to initiate convection would be easily met, and thus precipitation over the sea would similarly increase in intensity. The Southeast, which lies on a convective

margin, is shown to be opposite the Caribbean in the RSM. The "upped-ante" effect can also be reasonably assumed to explain drying seen in peninsular Florida in the CCSM3, though it cannot be considered the sole cause of drying.

The other mechanism responsible for the projected drying is expansion of the NASH. Observations over the past 30 years have indicated a westward expansion of the NASH over the Southeast. CCSM3 projects a continued expansion of the NASH over the Southeast that seems consistent with observations. Westward expansion of the NASH helps to stabilize the region, as seen through increased seasonal mean lifted index, which symptomatically carries additional precipitable water in the atmosphere. It is possible that this additional atmospheric precipitable water can drive a positive feedback forcing of temperatures, further warming the troposphere, though this hypothesis is not explicitly analyzed in this study.

4.2 Implications & Future Work

This study outlines plausible explanations for a changing precipitation climate over the Southeast in the late 21st century. The patterns seen in our global and regional climate projections are not assumed to be wholly accurate, but the mechanisms are at least physically plausible. This is supported by the fact that the proposed mechanisms are currently observed physical phenomena in the atmosphere. The impact of drying on the Southeast, especially during its wet season, could present difficulties for its inhabitants. Impacts include saltwater intrusion into the aquifers and an inability to meet the water needs of a growing population and a booming agricultural system.

Future work on this topic should consider other climate scenarios beyond A2. It is possible that more conservative estimates of CO_2 emission will produce a different response, especially considering that increasing GHG concentrations likely drives both mechanisms. Also, future work should also involve a synthesis of multiple models. Specifically, more modern models (particularly models from CMIP5) should be considered and their projections analyzed. The RSM can be forced with any model, so downscaling the global models to the regional domain is feasible for any models available. Likewise, other regional models should be considered, as the results can differ between them. A synthesis of multiple models should be able

to provide a convincing estimate of each mechanism's contributions to precipitation change and establish a possible range of outcomes for rainfall over the Southeast.

REFERENCES

Atkins, N. T., R. M. Wakimoto, and T. M. Weckwerth, 1995: Observations of the Sea-Breeze Front during CaPE. Part II: Dual-Doppler and Aircraft Analysis. *Mon. Wea. Rev.*, **123**, 944-969.

Biggs, W. G., and M. E. Graves, 1962: A Lake Breeze Index. *J. Appl. Meteor. Climatol.*, **1**, 474-480.

Briegleb, B. P., C. M. Bitz, E. C. Hunke, W. H. Lipscomb, M. M. Holland, J. L. Schramm, and R. E. Moritz, 2004: Scientific description of the sea ice component in the Community Climate System Model, Version Three. Tech. Rep. NCAR/TN-463+STR, 78 pp.

Carbone, R. E., and J. D. Tuttle, 2008: Rainfall Occurrence in the U.S. Warm Season: The Diurnal Cycle. *J. Climate,* **21**, 4132-4146.

Chan, S. C., V. Misra, 2010: A diagnosis of the 1979-2005 extreme rainfall events in the Southeastern United States with isentropic moisture tracing. *Mon. Wea. Rev*., **138**, 1172-1185.

Chiang, J. C. H., and A. H. Sobel, 2002: Tropical tropospheric temperature variations caused by ENSO and their influence on the remote tropical climate, *J. Climate*, **15,** 2616 – 2631.

Chou, M.D., and K. T. Lee 1996: Parameterizations for the absorption of solar radiation by water vapor and ozone, *J. Atmos. Sci*., **53,** 1203–1208.

Chou, M.D., and M. J. Suarez, 1994: An efficient thermal infrared radiation parameterization for use in General Circulation Models, NASA Tech. Rep. Ser. Global Mod. Data Assimilation, 85 pp.

Christensen, J. H., and Coauthors, 2007: Regional climate projections. Climate Change 2007: The Physical Science Basis, S. Solomon et al., Eds., Cambridge University Press, 847–94.

Clement, A. C., A. C. Baker, and J. Leloup, 2010: Climate change: Patterns of tropical warming. *Nat. Geosci*., **3,** 8–9.

Collins, W. D., and Coauthors, 2004: Description of the NCAR Community Atmosphere Model (CAM3). Tech. Rep. NCAR/TN-464+STR, 226 pp.

Collins, W. D., and Coauthors, 2006: The Community Climate System Model Version 3 (CCSM3). *J. Climate*, **19,** 2122–2143.

Collins, W. D., and Coauthors, 2006a: The formulation and atmospheric simulation of the Community Atmosphere Model version 3 (CAM3). *J. Climate*, **19,** 2144–2161.

Dai, A., 2006: Precipitation characteristics in eighteen coupled climate models. *J. Climate*, **19,** 4606-4630.

DeGaetano, A. T. and R. J. Alen, 2002: Trends in twentieth-century temperature extremes across the United States. *J. Climate*, **15,** 3188-3205.

Dickinson, R. E., K. W. Oleson, G. Bonan, F. Hoffman, P. Thornton, M. Vertenstein, Z.-L. Yang, and X. Zeng, 2006: The Community Land Model and its climate statistics as a component of the Community Climate System Model. *J. Climate*, **19,** 2302–2324.

Ek, M. B., K. E. Mitchell, Y. Lin, E. Rogers, P. Grunmann, V. Koren, G. Gayno, and J. D. Tarpley 2003: Implementation of Noah land surface model advances in the National Centers for Environmental Prediction operational mesoscale Eta model, *J. Geophys. Res.*, **108**, 8851.

Greene, D. R., and Hudlow, M. D. 1982: Hydrometeorologic Grid Mapping Procedures. AWRA International Symposium on Hydrometeorology, Denver, CO, 598 pp.

Hansen, J. W., A. W. Hodges, and J. W. Jones, 1998: ENSO Influences on Agriculture in the Southeastern United States. *J. Climate*, **11**, 404–411.

Hong, S. Y., and H. L. Pan, 1996: Nonlocal boundary layer vertical diffusion in a medium range forecast model, *Mon. Weather Rev*., **124,** 2322–2339.

Juang, H. H., and M. Kanamitsu, 1994: The NMC Nested Regional Spectral Model. *Mon. Wea. Rev*., **122,** 3-26.

Kanamaru, H., and M. Kanamitsu, 2007: Scale selective bias correction in a downscaling of global analysis using a regional model, *Mon. Weather Rev*., **135,** 334–350.

Kanamitsu, M., W. Ebisuzaki, J. Woollen, S. K. Yang, J. J. Hnilo, M. Fiorino, and G. L. Potter, 2002: NCEP DOE AMIP II reanalysis (R2), *Bull. Am. Meteorol. Soc*., **83,** 1631–1643.

Karl, T. R., H. F. Diaz, and G. Kukla, 1988: Urbanization: Its detection and effect in the United States Climate Record, *J. Climate*, **1,** 1099-1123.

Karl, T. R., J. M. Melillo and T. C. Peterson, 2009: Global Climate Change Impacts in the United States, Cambridge University Press, 188 pp.

Katz, R. W., M. B. Parlange, and C. Tebaldi, 2003: Stochastic modeling of the effects of large-scale circulation on daily weather in the southeastern U.S. *Climatic Change*, **60,** 189–216.

LeMone, M. A, 1973: The Structure and Dynamics of Horizontal Roll Vortices in the Planetary Boundary Layer. *J. Atmos. Sci.*, **30**, 1077–1091.

Li, W., L. Li, R. Fu, L. Deng, and H. Wang, 2011: Changes to the North Atlantic Subtropical High and its Role in the Intensification of Summer Rainfall Variability in the Southeastern United States. *J. Clim*ate, **24,** 1499-1506.

Liang, X.-Z., J. Pan, J. Zhu, K. E. Kunkel, J. X. L. Wang, and A. Dai, 2006: Regional climate model downscaling of the U.S. summer climate and future change, *J. Geophys. Res*., **111**.

Lin, Y. and K. E. Mitchell, 2005: The NCEP Stage II/IV hourly precipitation analyses: development and applications. Preprints, 19th Conf. on Hydrology, American Meteorological Society, San Diego, CA, 9-13 January 2005, Paper 1.2.

Loveland, T. R., J. W. Merchant, B. C. Reed, J. F. Brown, D. O. Ohlen, P. Olson, and J. Hutchinson, 1995: Seasonal land cover regions of the United States, *Ann. Assoc. Am. Geogr.,* **85**, 339–355.

Mearns, L.O. Et al., 2007, updated 2011. The North America Regional Climate Change Assessment Program dataset, National Venter for Atmospheric Research Earth System Grid data portal, Boulder, CO. Data downloaded 2012-02-27.

Misra, V., and coauthors, 2011: Climate Scenarios: A Florida-Centric View, Florida Climate Change Task Force, 61 pp.

Misra, V., L. Moeller, L. Stefanova, S. Chan, J. J. O'Brien, T. J. Smith III, and N. Plant, 2011a: The influence of the Atlantic Warm Pool on the Florida panhandle sea breeze, *J. Geophys. Res*., **116,** doi**:**10.1029/2010JD015367.

Nakicenovic, N., and R. Swart, 2000: Special Report on Emissions Scenarios. Cambridge University Press, 612 pp.

Oleson, K. W., and Coauthors, 2004: Technical description of the Community Land Model (CLM). Tech. Rep. NCAR/TN-461+STR, 174 pp.

Ortegren J.T., P. A. Knapp, J. T. Maxwell, W. P. Tyminski, and P. T. Soule, 2011: Ocean-Atmosphere Influences on Low-Frequency Warm-Season Drought Variability in the Gulf Coast and Southeastern United States. *J. App. Meteor. Climatol.*, **50,** 1177-1186.

Pan, Z., R. W. Arritt, E. S. Takle, W. J. Gutowski Jr., C. J. Anderson, and M. Segal, 2004: Altered hydrologic feedback in a warming climate introduces a "warming hole." *Geophys. Res. Lett.*, **31**, doi:10.1029/2004GL020528.

Parker, M.D. and D.A. Ahijevych, 2007: Convective episodes in the east-central United States. *Mon. Wea. Rev.*, **135**, 3707-3727.

Portmann, R. W., S. Solomon, and G. C. Hegel, 2009: Spatial and seasonal patterns in climate change, temperatures, and precipitation across the United States. *Proc. Natl. Acad. Sci. U. S. A.,* **106**, 8441-8446, doi:10.1073/pnas.0901736106.

Rauscher, Sara A., Fred Kucharski, David B. Enfield, 2011: The Role of Regional SST Warming Variations in the Drying of Meso-America in Future Climate Projections. *J. Climate*, **24,** 2003–2016.

Robinson, W. A., R. Reudy, and J. E. Hansen 2002: General circulation model simulations of recent cooling in the east-central United States. *J. Geophys. Res.*, **107,** doi:10.1029/2001JD001577.

Schwartz, B. E., and L. F. Bosart, 1979: The Diurnal Variability of Florida Rainfall. *Mon. Wea. Rev.,* **107**, 1535-1545.

Seager, R., A. Tzanova, J. Nakamura, 2009: Drought in the Southeastern United States: Causes, Variability over the Last Millennium, and the Potential for Future Hydroclimate Change. *J. Climate*, **22,** 5021–5045.

Seager, R., N. Naik, and L. Vogel, 2011: Does global warming cause intensified interannual hydroclimate variability?. *J. Climate*, in press.

Simpson, J. E., 1994: Sea Breeze and Local Winds. Cambridge Univ. Press, 234 pp.

Slingo, J. M. 1987: The development and verification of a cloud prediction scheme for the ECMWF model. *Q. J. R. Meteorol. Soc.*, **113,** 899–927.

Smith, R. D., and P. R. Gent, 2002: Reference manual for the Parallel Ocean Program (POP), ocean component of the Community Climate System Model (CCSM2.0 and 3.0). Tech. Rep. LA-UR-02-2484, Los Alamos National Laboratory. [Available online at http://www.ccsm.ucar.edu/models/ccsm3.0/pop.]

Stefanova, L., V.Misra, S. C. Chan, M. Griffin, J. J. O'Brien, and T. J. Smith III, 2011: A proxy for high-resolution regional reanalysis for the Southeast United States. *Climate Dyn.*, in print.

Wallace, J. M., 1975: Diurnal Variations in Precipitation and Thunderstorm Frequency over the Conterminous United States. *Mon. Wea. Rev.,* **103**, 406-419.

Wang, C., and D. B. Enfield, 2001: The tropical western hemisphere warm pool. *Geophys. Res. Lett*., **28,** 1635–1638.

Willmott, C. J., and K. Matsuura, 2000: Terrestrial air temperature and precipitation: Monthly and annual climatologies, [Available online at http://climate.geog.udel.edu/climate.]

Xie, S., C. Deser, G. A. Vecchi, J. Ma, H. Teng, A. T. Wittenberg, 2010: Global Warming Pattern Formation: Sea Surface Temperature and Rainfall. *J. Climate*, **23,** 966–986.

BIOGRAPHICAL SKETCH

Christopher Selman was born in Bradenton, Florida in 1986. All his life he had been interested in meteorology, and in the Fall of 2005 he began studying at the Florida State University. He completed his degree in meteorology in Spring of 2009, and began his graduate studies again at the Florida State University, under the guidance of Dr. Vasu Misra on the topic of diurnal variation and seasonal climatology. This thesis is in partial fulfillment of an M.S. in meteorology, with an expected completion date of Summer 2012. Upon completion of the M.S., Christopher will continue studying diurnal variations of rainfall under Dr. Vasu Misra, for a PhD in meteorology.